INTERACTIONS OF SYNTHETIC METAL PORPHYRINATES WITH PHUS, A CYTOPLASMIC HEME TRAFFICKING PROTEIN FROM *PSEUDOMONAS AERUGINOSA*

A Thesis
Submitted to the Graduate Faculty
of the
North Dakota State University
of Agriculture and Applied Science

By

Amber Elise Moberg

In Partial Fulfillment of the Requirements
for the Degree of
MASTER OF SCIENCE

Major Department:
Chemistry and Biochemistry

August 2010

Fargo, North Dakota

North Dakota State University

Graduate School

Title

Interactions of Synthetic Metal Porphyrinates with PhuS, a Cytoplasmic Heme Trafficking Protein from *Pseudomonas aerugiosa*

By

Amber Elise Moberg

The Supervisory Committee certifies that this ***disquisition*** complies with North Dakota State University's regulations and meets the accepted standards for the degree of

MASTER OF SCIENCE

ABSTRACT

Moberg, Amber Elise, M.S., Department of Chemistry and Biochemistry, College of Science and Mathematics, North Dakota State University, August 2010. Interactions of Synthetic Metal Porphyrinates with PhuS, a Cytoplasmic Heme Trafficking Protein from *Pseudomonas aeruginosa.* Major Professor: Dr. Kenton R. Rodgers.

Pseudomonas aeruginosa is an opportunistic, Gram negative, bacterial pathogen that commonly establishes infection in immunocompromised individuals. It contains protein-based, iron uptake pathways that target both heme and nonheme iron sources in the host. When the ***Pseudomonas*** **h**eme **u**ptake system is compromised by genetic knockout of the cytoplasmic heme trafficking protein, PhuS, the ability to establish infection is lost. PhuS functions to transfer heme to a heme oxygenase, an O_2 dependent heme metabolizing enzyme, so that it can be degraded to a usable form for the organism. Within the long-term goal of developing pharmaceutical agents to inhibit heme uptake by bacterial pathogens, this study aims to evaluate the general thermodynamic parameters of metalloporphyrin binding to PhuS. Two synthetic iron porphyrinates and the Ni(II) complex of protoporphyrin IX have been investigated and their binding constants have been determined. The implications of these results for inhibiting heme uptake will be discussed.

ACKNOWLEDGEMENTS

I would like to thank everyone that has helped me along the process of receiving my degree. I would especially like to thank my family, boyfriend, and friends for always supporting me and being there for me. I would also like to thank Dr. Rodgers for all of his help and support throughout this process, as well as the rest of my committee: Dr. Lukat-Rodgers, Dr. Offerdahl, and Dr. Pruess. I would like to thank my lab-mates that I worked with throughout my time here: Darci, Bridget, Katrina, and Erin. I would also like to thank the Department of Chemistry and Biochemistry, in particular Wendy and Greg, for all of their help.

Overall I believe that attending graduate school at NDSU was a good fit for me. This academic institution provided me with excellent work experience as well as life experience. I am coming out of my education here with a much different outlook upon life, as well as different career goals than two years ago when I first began. I am glad that I was able to experience going to graduate school, and I am also glad that I had the opportunity to interact with so many great people in my short time here.

TABLE OF CONTENTS

ABSTRACT..... iii

ACKNOWLEDGEMENTS..... iv

LIST OF TABLES..... viii

LIST OF FIGURES..... ix

LIST OF EQUATIONS..... xi

LIST OF ABBREVIATIONS..... xii

CHAPTER 1: A SURVEY OF BACTERIAL IRON ACQUISITION..... 1

Introduction..... 1

The Gram Stain..... 1

Environmental Iron..... 2

Toxicity of Iron..... 3

Iron within Biological Systems..... 3

Forms of Iron in Biological Systems..... 5

Spectroscopy of Metalloporphyrins..... 6

Host Combatant of Bacterial Iron Acquisition..... 7

Introduction to Bacterial Iron Acquisition..... 7

Iron Transportation through the Outer Membrane..... 9

Direct Heme Uptake Systems..... 15

Iron Transportation in the Periplasm..... 17

Iron Transportation through the Inner Membrane..... 18

Iron Transportation and Degradation in the Cytoplasm..... 19

Iron Acquisition of *Pseudomonas aeruginosa*..... 22

PhuS..... 24

Goals of this Study..... 26

References..... 27

CHAPTER 2: MATERIALS AND METHODS..... 35

Introduction..... 35

The pET Plasmid as an Expression Vector in *E. coli*..... 35

Preparation of the pET21 BL21(DE3) *E. coli* Cells..... 37

Preparation of PhuS..... 37

FeTPPS Synthesis..... 39

FeTMPyP Synthesis..... 42

Ni(II)PPIX..... 44

Spectrophotometric Titrations..... 44

Global Analysis Fitting Software..... 46

References..... 47

CHAPTER 3: RESULTS OF PHUS TITRATIONS WITH FETPPS AND FETMPYP..... 49

Introduction..... 49

Results..... 53

Discussion..... 58

References..... 59

CHAPTER 4: RESULTS OF NI(II)PPIX TITRATIONS WITH PHUS..... 63

Introduction..... 63

Results..... 66

Discussion..... 75

References.. 76

LIST OF TABLES

Table		Page
1.1	Comparison of known Gram negative Group II Ton-B dependent outer membrane heme receptors, their substrates, and conserved residues and motifs	16
1.2	Gram negative cytoplasmic binding proteins	21
3.1	Average stability constants of binding FeTPPS and FeTMPyP to PhuS determined through nonlinear least squares fit analysis	57
4.1	Average apparent stability constants for the Ni(II)PPIX:PhuS complex	74

LIST OF FIGURES

Figure		Page
1.1	Cross section of the membrane structure of a Gram negative bacterium	2
1.2	The Fenton reaction	3
1.3	Structure of heme b	4
1.4	Ligand field splitting diagrams for high and low spin Fe(II) and Fe(III)	5
1.5	Example of UV-visible spectroscopy of metalloporphyrins	6
1.6	General scheme for direct uptake of host heme into a Gram negative organism	8
1.7	Three types of siderophore functional groups	10
1.8	FpvA receptor of *P. aeruginosa* bound to its siderophore, pyoverdine	11
1.9	Cartoon representation of the Has system	12
1.10	HasA transfer of heme to HasR in *S. marcesens*	13
1.11	Heme binding residues of ShuA from *S. dysenteriae*	17
1.12	Regiospecific degradation of heme by heme oxygenase	20
1.13	Cartoon representation of the *Phu* system of *P. aeruginosa*	23
1.14	Homology structure of PhuS derived from ChuS in *Eschericia coli*	25
1.15	Illustration of the *Phu* operon from *P. aeruginosa*	25
1.16	Cartoon illustration of the molecularities of holo and half-holo PhuS	26
2.1	Typical UV-visible absorbance spectra of PhuS	38
2.2	Synthesis reactions of FeTPPS and FeTMPyP	40
2.3	Labeled ^{1}H NMR spectra for FeTPPS	41
2.4	Labeled ^{1}H NMR spectra for FeTMPyP	43

2.5 UV-visible absorbance spectra for metalloporphyrins..... 45

3.1 Acid base speciation of FeTPPS 51

3.2 Acid base speciation of FeTMPyP..... 52

3.3 UV-visible spectra for the titration of PhuS with FeTPPS and Global fitting analysis..... 54

3.4 UV-visible spectra for the titration of PhuS and FeTMPyP and Global fitting analysis..... 56

4.1 Stick structure of Ni(II)PPIX..... 64

4.2 Ligand field splitting diagram for square planar d^8 complexes..... 65

4.3 UV-visible absorbance spectra of Ni(II)PPIX in aqueous solution over time..... 67

4.4 UV-visible spectra for the titration of PhuS and Ni(II)PPIX..... 68

4.5 Global fitting analysis of the titration of PhuS with Ni(II)PPIX..... 70

4.6 Plot of molar absorptivity at 401 nm versus high concentration of Ni(II)PPIX in aqueous solution..... 71

4.7 UV-visible spectrum of dilute Ni(II)PPIX in aqueous solution..... 72

4.8 UV-visible difference spectrum of PhuS titrated with Ni(II)PPIX..... 73

4.9 Global analysis of PhuS titrated with Ni(II)PPIX 74

LIST OF EQUATIONS

Equation Page

4.1 Fitting function for dimeric constant calculation of Ni(II)PPIX..... 71

LIST OF ABBREVIATIONS

ADP	adenosine diphosphate
Apo	without heme
ATP	adenosine triphosphate
CBP	cytoplasmic binding protein
DME	dimethyl ester
DMSO	dimethyl sulfoxide
DNA	deoxyribonucleic acid
FeTMPyP	5,10,15,20-tetrakis(N-methyl-4'-pyridyl) porphyrinato iron (III) chloride
FeTPPS	5,10,15,20-tetrakis(4-hydryl-sulfonatophenyl) porphyrinato iron (III) chloride
FDA	food and drug administration
FUR	ferric uptake repressor
Has	heme acquisition system
Hb	hemoglobin
HO	heme oxygenase
Holo	with heme
Hp	haptoglobin
HPLC	high performance liquid chromatography
Hx	hemopexin
IPTG	isopropyl β-D-1-thiogalactopyranoside
kDa	kilodalton
LB	lysogeny broth
Mb	myoglobin

NADPH	nicotinamide adenine dinucleotide phosphate
NiPPIX	nickel (II) protoporphyrin IX
NMR	nuclear magnetic resonance
PBP	periplasmic binding protein
PDT	photodynamic therapy
PMSF	phenylmethylsulfonyl fluoride
TMPyP	meso-tetra (N-methyl-4-pyridyl) porphine tetra tosylate
TPPS	meso-tetra (4-sulfonatophenyl) porphine dihydrochloride
Tris	2-amino-2-hydroxymethyl-propane-1,3-diol
UV	ultraviolet

CHAPTER 1: A SURVEY OF BACTERIAL IRON ACQUISTION

Introduction

With the exception of a few species of lactic acid producing bacteria, such as lactobacilli, bacterial organisms have been found largely to be iron limited.[1] Bacteria go to great lengths to obtain iron from their environment through the development of complex pathways in order to acquire this necessary resource. Bacterial pathogens obtain iron from the host's store of the element. Therefore understanding the iron-uptake systems of pathogenic bacteria is important to human health. Any avenue of these pathways has the potential to be of interest in the pursuit of pharmaceuticals used to inhibit infection of pathogenic bacteria.

The focus for this thesis is the binding logistics of synthetic metalloporphyrins to PhuS, a protein within the direct heme uptake system of the Gram negative bacterium, *Pseudomonas aeruginosa*. Therefore this review touches upon the various systems that Gram negative bacteria use to obtain iron from their environment. The goal of this introduction is to summarize what is known about how these systems of proteins function to acquire iron in the host environment. The ultimate goal of this work is to understand the thermodynamic and mechanistic aspects of heme binding to these proteins with an eye toward discovering pharmaceutical agents to inhibit bacterial heme uptake pathways.

The Gram Stain

Bacteria can be subdivided into two groups through the application of the Gram staining technique.[2] The first group produces a purple color upon completion of the staining protocol and is known as Gram positive.[2] Gram positive bacteria contain one outer membrane as well as a thick outer peptidoglycan layer that encompasses the outside

of the organism.[2] The second group stains pink upon completion of the Gram staining technique and is known as Gram negative.[2] Figure 1.1 shows a cartoon structure of the basic physiology of a Gram negative bacterium. Gram negative bacteria stain pink because they are composed of two membranes with a peptidoglycan layer occurring in the periplasmic space.[2] These membranes and peptidoglycan layer provide a protective barrier for the bacterium as well as the matrix for an elaborate protein importation and exportation system through which the bacterium can obtain its required nutrients and detoxify itself. Because these two groups of bacteria differ in their membrane composition, they have developed diverse means for obtaining iron from their environments. The Gram negative organism's mechanism is generally more complex as it requires transportation of iron across two membranes instead of just one as in Gram positive bacteria. This first chapter focuses largely on Gram negative bacterial iron acquisition.

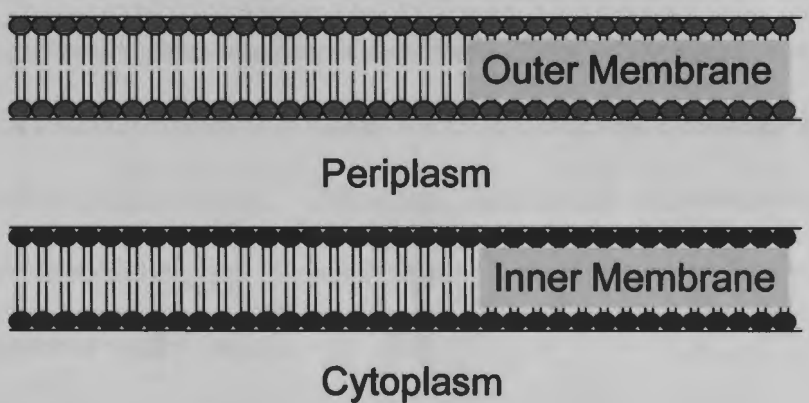

Figure 1.1. Cross section of the membrane structure of a Gram negative bacterium. Both membranes are composed of a phospholipid bilayer that houses various bacterial proteins and is permeable via diffusion for small molecules. The area in between the two membranes is composed largely of peptidoglycan and denoted the periplasm. The area inside of the inner membrane is known as the cytoplasm.

Environmental Iron

Iron is the fourth most abundant element in the Earth's crust, but it is not readily bioavailable because it is found mostly in an insoluble form.[3] Free iron(III) in solution is

found at about 10^{-18} M in the environment and within the mammalian host. [3] In order for iron-limited bacteria to thrive, intracellular concentrations of iron must reach micromolar levels.[3]

Toxicity of Iron

Iron is toxic to cells if it is free in solution.[4] In the presence of hydrogen peroxide ferrous iron reacts with hydrogen peroxide to form free radicals such as the hydroxyl radical via the Fenton reaction (Fig. 1.2), which can damage biomacromolecules, such as nucleic acids, proteins, carbohydrates, and lipids.[4]

$$Fe^{+2} + H_2O_2 \rightarrow Fe^{+3} + OH^- + OH\bullet$$

Figure 1.2. The Fenton Reaction. Fe(II) is oxidized to Fe(III) by hydrogen peroxide creating hydroxide and the hydroxyl radical as byproducts.

In order to minimize these adverse interactions, virtually all *in-vivo* iron is sequestered in proteins such as transferrin, lactoferrin, ferritin, and heme proteins amongst others.[5] Despite its toxic effects, iron makes for an effective redox mediator because it can be found in several oxidation states.[5] This makes it suitable for such processes as electron transport, peroxide reduction, and oxygen activation for procedures such as nucleotide and hormone biosynthesis within the cell.

Iron within Biological Systems

Iron containing proteins in mammalian hosts fall into two categories: heme-containing proteins, and non-heme iron proteins. The most abundant of the heme containing proteins is hemoglobin, which is present at approximately 15 grams per 100 milliliters of blood.[6] It is composed of four subunits, each containing one molecule of heme. Figure 1.3 shows the *b*-type heme which is an aromatic, 22 π electron, macrocyclic

ring. This ring gives heme its chromophoric properties, providing its characteristic red coloration.

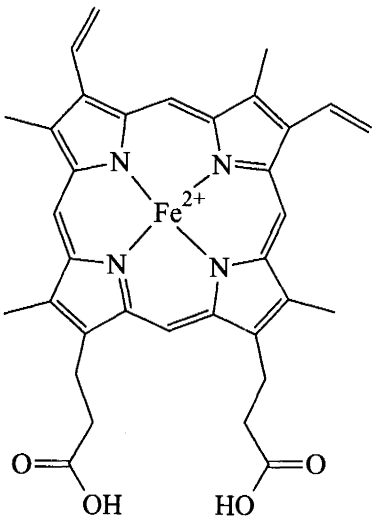

Figure 1.3. Structure of heme b. Heme b is the mammalian host heme contained in hemoglobin. In heme b iron is bonded to the four pyrrolic nitrogens in the protoporphyrin IX ring. The ring contains vinyl, methyl, and propionate functional groups, which have a pK_a of 4.87.[7] In hemoglobin, Fe(II)PPIX is bonded to the protein through the imidazole side chain of an axial histidine ligand.[6] Heme b outside of hemoglobin is readily oxidized to form ferriprotoporhyrin IX. Bacterial receptors have been shown to bind this form of heme.[8]

Hemoglobin has a dissociation constant for heme of 10^{-12} to 10^{-15} M.[9] Some other sources of heme in host proteins include myoglobin, hemopexin, and human serum albumin, which have dissociation constants for heme of 10^{-14}, 10^{-13}, and 10^{-8} respectively.[5, 8] Some examples of non-heme containing proteins are ferritin, transferrin, and lactoferrin. Ferritin is an iron storage molecule that is able to hold 4,500 atoms of iron per mol.[8] It stores iron as hematite which is a poor resource for bacterial acquisition of iron because it has a solubility product constant of 10^{-38} M.[5] Transferrin acts as a scavenger for free iron in the serum, and lactoferrin scavenges free iron in the lymphatic system and mucosal secretions.[5] These proteins have affinity constants for iron(III) of 10^{-13} M.[5] Transferrin functions to

release iron in acidic endosomes, so when the pH is lowered sufficiently it undergoes an allosteric transition to release its iron.[10] However lactoferrin has the capacity to bind free iron down to a pH of 3.5.[10]

Forms of Iron in Biological Systems

Iron is found in a variety of oxidation and spin states depending on the environment that it is contained in and what ligands are bound to it. This introduction focuses on Fe(II) and Fe(III), although the more highly oxidized Fe(IV) and Fe(V) oxidation states are known to play important roles in biocatalysis. Figure 1.4 shows the ligand field splitting diagrams for the *d* orbitals in high spin Fe(II) and Fe(III). The two synthetic

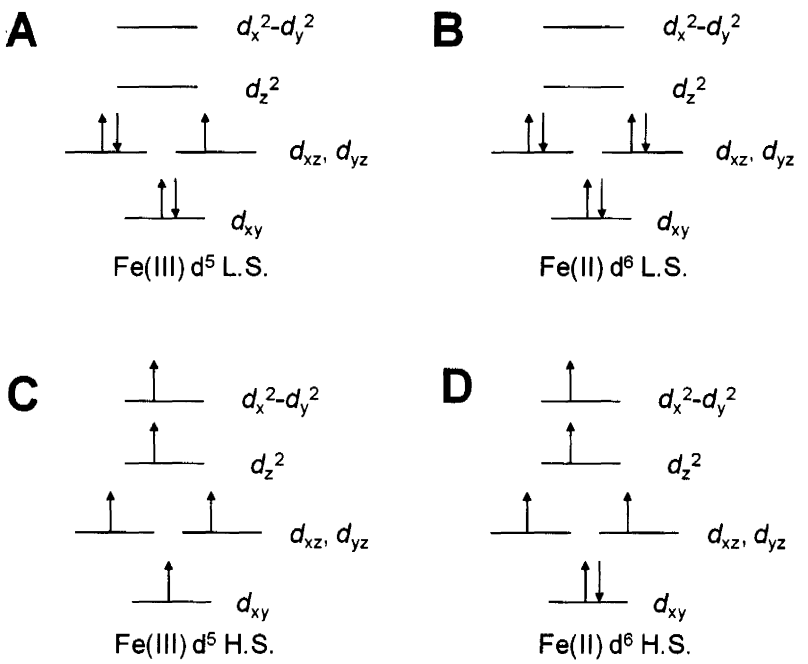

Figure 1.4. Ligand field splitting diagrams for high and low spin Fe(II) and Fe(III). A) Low spin Fe(III) has 5 electrons in its outer shell *d* orbitals, with one unpaired electron. B) Low spin Fe(II) contains 6 electrons in its outer shell *d* orbitals with no unpaired electrons. C) High spin Fe(III) contains five electrons in its outer shell *d* orbitals that are all unpaired. D) High spin Fe(II) contains six electrons in its outer shell *d* orbitals, with four of these being unpaired.

metalloporphyrins, whose binding to PhuS was investigated in this study, are both high spin Fe(III) complexes.

Spectroscopy of Metalloporphyrins

Iron porphyrins, as well as other metalloporphyrin complexes, exhibit characteristic spectroscopic features that are detectable via UV-visible spectroscopy. Figure 1.5 shows a typical metalloporphyrin UV-visible absorbance spectrum using Ni(II)PPIX as a example. Metalloporphyrins exhibit a large absorbance band known as the Soret band or B-band, which is attributable to the π-π^* transition from the singlet ground state to the second singlet excited state.[11] Typically metalloporphyrins exhibit α and β bands as well which can also be denoted as Q(0,0) and Q(0,1) bands respectively. These bands arise from the

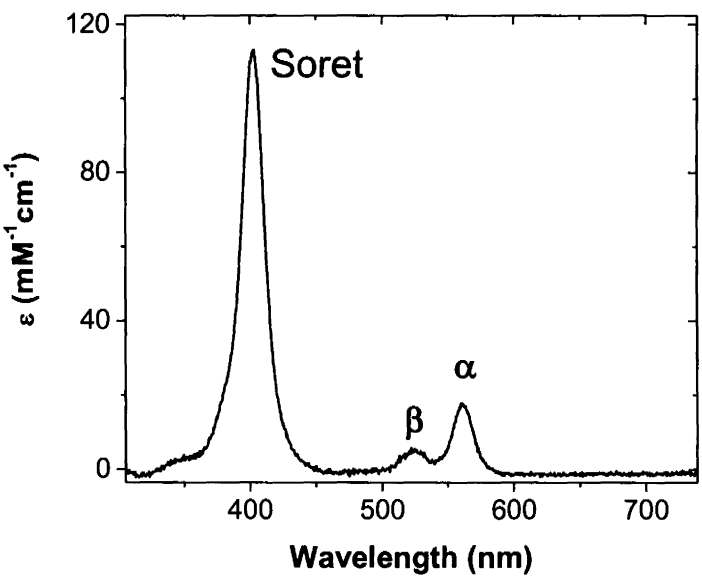

Figure 1.5. Example of UV-visible spectroscopy of metalloporphyrins. Depicted is a plot of molar absorptivity coefficient versus wavelength denoting the characteristic bands of metalloporphyrin species.

π-π^* transition from the singlet ground state to the first singlet excited state (α) and its vibronic side band (β).[11]

Host Combatant of Bacterial Iron Acquisition

Bacteria have developed means for scavenging iron from the host's iron containing proteins, but the host is not willing to give up this precious resource without a fight. The host has developed defense mechanisms for fighting bacterial infections by withholding iron.[10] The host and bacterium are in constant combatant over iron as bacteria are evolving new ways to obtain this necessary element. For example some species of bacteria are able to lower the pH of the host environment which causes transferrin to release its iron.[10] The human body responds to the invasion of bacteria by decreasing the amount of iron that is present by absorbing less iron as well as reducing the amount of iron that is available in the plasma around the infection.[10] The liver secretes the protein hepcidin in order to regulate the amount of iron present in the plasma.[12] There is an increase in hepcidin synthesis and macrophage ferritin which stops macrophages from discharging iron.[10] Lactoferrin is released from neutrophil granules, and haptoglobin and hemopexin are released from the hepatic system to sequester free iron, hemoglobin, and hemin respectively.[10]

Introduction to Bacterial Iron Acquistion

Iron, in the form of heme within the host, is solubilized by an abundance of proteins that create very stable complexes. Despite this abundance, the iron is not easy to attain, so bacteria have created specialized machinery to obtain this iron in order to establish infection. There are two different approaches that bacteria take in order to obtain iron, the first is through a receptor that recognizes a secreted bacterial agent such as a siderophore bound to iron(III) or a hemophore bound to heme. The second way that bacteria obtain iron is through a receptor that binds host heme and host-heme containing proteins. A general iron uptake system for receptor-based internalization of host heme is shown in

Figure 1.6. Heme is excised from a host protein by a Ton B dependent outer membrane receptor, whereupon it is actively transported through the outer membrane. The Ton B,

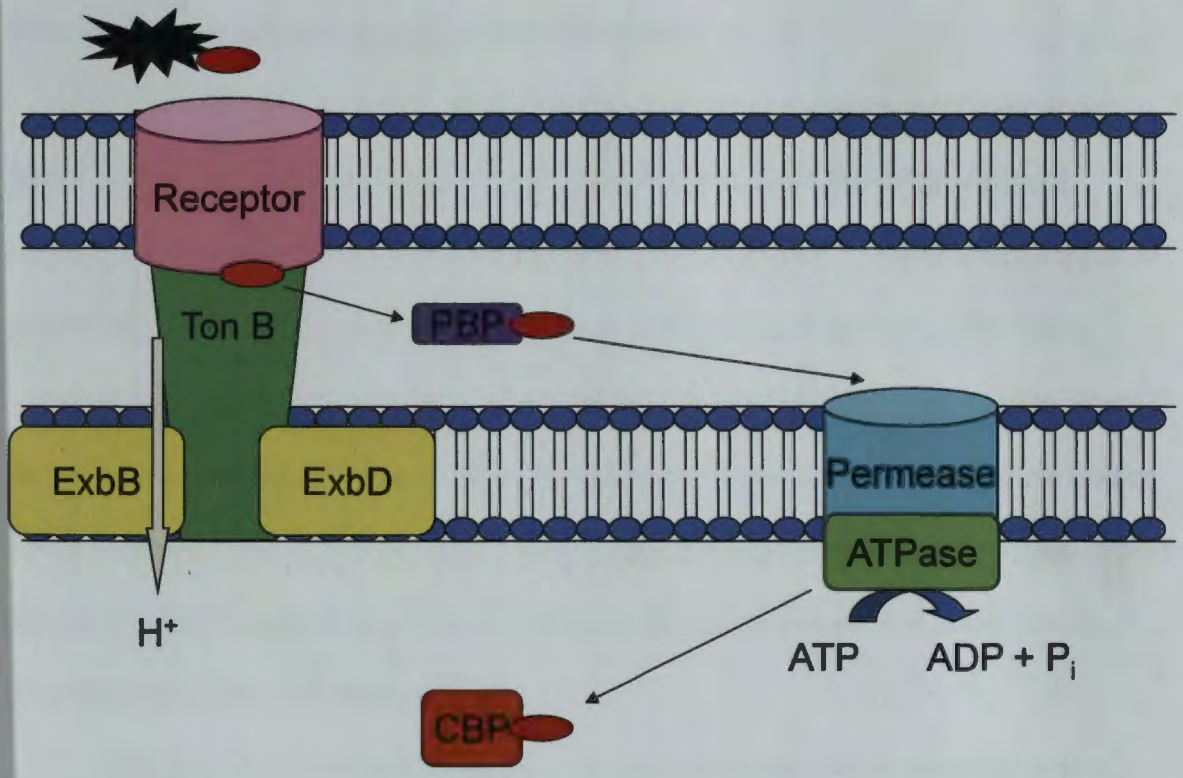

Figure 1.6. General scheme for direct uptake of host heme into a Gram negative organism. In this schema, heme is denoted by a red oval, which is transferred from a protein (black) to a receptor. PBP stands for periplasmic binding protein, and CBP denotes a cytoplasmic binding protein.

ExbB and ExbD proteins function as a complex to transduce the energy from the proton motive force across the inner membrane in order to bring heme through the outer membrane receptor. The iron is then passed to a periplasmic binding protein which traffics the heme to an inner membrane ABC transporter. The ABC transporter is composed of a permease and an ATPase which function to transport the heme through the inner membrane. The permease spans the membrane providing a channel for the passage of iron, and is composed of two domains. The ATPase functions to catalyze the hydrolysis of ATP

in order to provide the energy to transport heme across the inner membrane. The heme is then transferred to a cytoplasmic heme trafficking protein.

Iron Transportation through the Outer Membrane

Because diffusion of siderophores and heme through the outer membrane is not facile and because iron levels must be tightly regulated to avoid the aforementioned cellular damage, they are actively transported through a receptor.[13] There are two types of outer membrane receptors denoted Groups I and II that Gram negative bacteria use to transport iron through the outer membrane. Group I outer membrane receptors recognize the iron(III) complexes of secreted siderophores and heme-loaded, secreted protein known as hemophores.[13] Group II outer membrane receptors recognize host heme proteins. These two groups range in size from 70 to 120 kDa, and they work to transport heme into the periplasm via a Ton B dependent process.[13]

Homology between various Ton B dependent receptors is low other than at the highly conserved N-terminus, yet interestingly these receptors exhibit high structural similarity.[14] The receptors have a β-barrel structure that is composed of 22 β strands.[14-15] They are tilted within the outer membrane and contain long loops on their exterior with short turns on the periplasmic side of the membrane.[14-15] These receptors have five conserved residues at their N-terminus which is known as the Ton B box, and these residues are part of the plug structure, which sits inside the barrel and prevents passive diffusion across the membrane.[14] Stabilization of this structure occurs due to hydrogen bonding and salt bridging between the barrel and the plug.[14-15] The plug sits on the inside of the β barrel and separates the outside of the receptor from the periplasmic space.[14] It is composed of a floor of β strands and loops with α helices.[14] The substrate that is specific to

the Ton B dependent outer membrane makes contact with the extracellular loops and apices at the top of the plug.[14] However the channel in the β-barrel with the plug is not large enough to pass the substrate, so the exact mechanism of transport is still not known.[15] It has been shown that substrate binding to the plug is able to trigger small conformational changes in the apices of the plug, while larger movements have been seen on the periplasmic side of the plug where the Ton B box is found.[14] Some examples of outer membrane receptors are FecA and FhuA in *Escherichia coli* which act to internalize siderophores.[15] HasR in *Serratia marcesens* and HxuC in *Haemophilus influenzae* are two examples of hemophore type Ton B dependent outer membrane receptors.[15]

Siderophores are low molecular weight compounds whose molecular weights are usually less than or equal to 1 kDa.[16] They are synthesized by nonribosomal peptide synthetases which resembles the same enzymatic machinery used for antibiotic synthesis.[5] The genes encoding for these siderophores are iron regulated, and the siderophore excretion mechanism is not known.[5] The structures of these siderophores are quite diverse, but they are all composed of three basic functional groups that are depicted in Figure 1.7.[17]

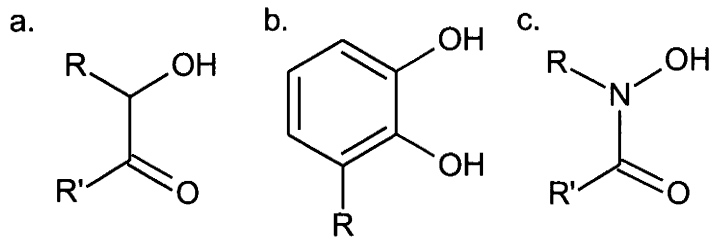

a.) Hydroxycarboxylic acid, b.) Catechol, c.) Hydroxamic acid

Figure 1.7. Three types of siderophore functional groups. Siderophores contain oxygen, nitrogen, or sulfur donor atoms.[17] These donor atoms create strong bonds with iron.[17] The functional groups are bidentate meaning that two oxygen atoms coordinate to Fe(III).[17]

Siderophores bind to Fe(III) with an affinity of about 10^{30} M^{-1} in a hexadentate

manner through the oxygen groups shown on the right hand side of each of these functional groups.[16] Fe(III) prefers to be coordinated in a octahedral ligand sphere, so it prefers to be bound to three of these functional groups.[16] Fe(III) is a hard metal ion so it preferentially binds hard oxygen atom based ligands.[17] Fe(II) is a softer metal so it favors softer ligands such as those that bind through nitrogen atoms.[17] Once iron is reduced to Fe(II), its affinity for the siderophore is greatly diminished and it is released from the complex. Because these complexes are so low in molecular weight, they are taken in through the receptor in the outer membrane as a whole.[16] Siderophores are targeted by specific Ton B dependent outer membrane receptors.[5] Two of the siderophores that *Pseudomonas aeruginosa* uses are pyoverdine and pyochelin. Figure 1.8 shows the cartoon structure of pyoverdine (red) bound to its β-barrel receptor FpvA.[17] *E. coli* uses the outer membrane receptors FhuA and FepA which uptake ferrichrome and ferrienterobactin respectively.[17]

Figure 1.8. FpvA receptor of *Pseudomonas aeruginosa* bound to its siderophore, pyoverdine.[18]

Hemophores are secreted molecules that either capture free heme or take it from host heme proteins such as hemoglobin. There are two types of hemophore systems, the

Has and Hxu systems. The Has system was first found in *S. marcesens* and shares 30 to 50% sequence homology with hemophore acquisition systems in other Gram negative bacteria.[8] A cartoon scheme of the Has system is shown in Figure 1.9.

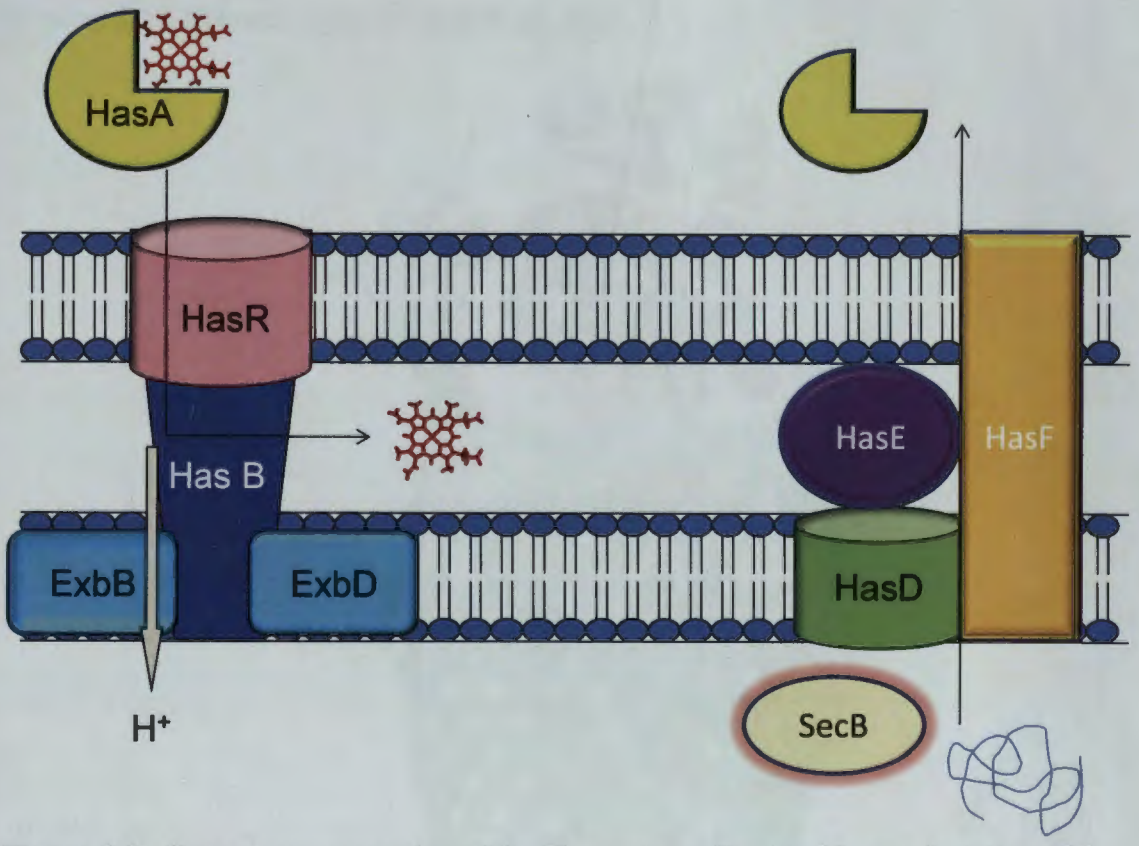

Figure 1.9. Cartoon representation of the Has system. Depicted is an adaptation of the Has system from Wandersman et. al. 2004.[5] The red structure bound to HasA represents heme from hemoglobin. The unfolded protein within the cytoplasmic space represents HasA before it has been secreted outside of the bacterium.

Once HasA bound to heme (holoHasA) comes upon the outer membrane receptor HasR, it forms a protein-protein complex that decreases the affinity of HasA for heme and allows it to be transported through HasR (Figure 1.10).[19] HasR internalizes heme in a HasB dependent manner. This active transport is powered by the inner membrane complex of HasB, ExbB, ExbD, which transduces the potential energy of the proton gradient (or proton motive force) across the inner membrane.[5] HasA is secreted by a three protein

system, composed of HasD, HasE, and HasF.[20] HasD is an ABC transporter, HasE is a membrane fusion protein, and HasF is a β-barrel protein that spans the inner and outer membranes.[20] SecB is a cytoplasmic chaperone that is necessary for excretion of HasA by keeping the c-terminal signal accessible on HasA.[21]

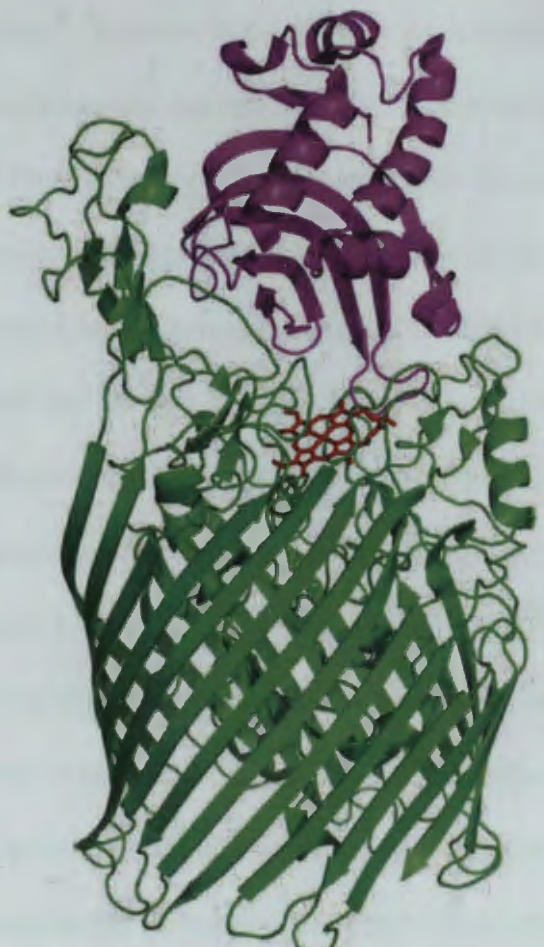

Figure 1.10. HasA transfer of heme to HasR in *S. marcesens*. Depicted is the crystal structure of the transfer of heme (red) from HasA (pink) to its receptor HasR (green).[22]

HasA is composed of seven β-strands that form an antiparallel β-sheet on one face and four α-helices on the other face.[23] Heme is held between two loops at the interface between the α and β fold.[23] In *S. marcesens*, the iron in heme is ligated by the unique axial ligand set, His32 and Tyr75.[24] It was found that these iron ligating histidine and tyrosine

amino acids were conserved in all species.[24] Based on carbon monoxide binding data the proposed mechanism for heme transfer from HasA to the receptor is that the His32 releases the heme first.[24]

HasR, the receptor for HasA, is proposed to be dependent on the Ton B homologue, denoted as HasB for energy.[25] Its barrel is predicted to be composed of a 99 residue aminoterminal extension with a plug domain and a β-barrel domain with a lumen that is then closed by a plug.[25] HasR is highly homologous to other heme and hemoprotein receptors.[26] It has the ability to take up free heme and hemoglobin with a dissociation constant of 10^{-6} M.[26] HasR takes up hemophore bound heme with a dissociation constant of 10^{-9} M, which is higher than HasA's dissociation constant of 10^{-11} M.[26] Caillet-Saguy predicted that upon binding to HasR the high-spin low-spin equilibrium is going to shift towards the high spin species.[19] This would cause HasA's affinity of heme to be lower than that of HasR and heme could then be passed to the receptor.[19]

The other type of hemophore system that has been identified, Hxu (heme/hemopexin utilization) is found in *H. influenzae*.[27] *H. influenzae* is unable to synthesize pyrrole rings so heme is its only source of protoporhyprin IX.[27] This hemophore system is composed of three proteins, HxuA, HxuB, and HxuC.[27] HxuA is a 99 kDa protein that is able to bind heme-hemopexin.[27] HxuB is proposed to release HxuA from the heme-hemopexin complex, and HxuC is the outer membrane receptor.[27] This system has not been found to be ubiquitously expressed, and in iron deplete conditions this hemophore system is not expressed at all.[27] The Hxu hemophore system is not as efficient as the Has system, but it allows for an increased range of substrates to be used to obtain iron.[27]

Direct Heme Uptake Systems

Iron, including heme uptake, is regulated by the Ferric Uptake Repressor (FUR).[28] These systems are similar in all bacteria.[29] FUR is composed of a 17 kDa homodimeric protein that binds to DNA at the operator region of the iron-dependent receptor genes when iron is replete in the system.[30] This binding represses transcription of the iron-dependent receptor genes.[28] When iron is depleted it dissociates from the homodimeric protein, thereby destabilizing its complex with DNA.[28] Then RNA polymerase is able to transcribe the iron-dependent receptor genes so that more iron can be taken into the bacterial system. FUR is thought to be ubiquitously expressed, and has been demonstrated to date in *Vibrio cholera, Yersinia pestis, Yersinia enterocolitica,* and *P. aeruginosa.*[8]

In order to obtain iron from the host medium, bacteria secrete hemolysin which lyses red blood cells and releases hemoglobin into the serum at 80-800 nM concentrations.[29] Hemoglobin is then picked up by haptoglobin, and heme is picked up by hemopexin or serum albumin.[29] Heme can then be taken up by a group II outer membrane receptor, a list of which is provided in Table 1.1. In *Y. enterocolitica* the outer membrane heme receptor is HemR.[31] In HemR heme binding involves His128 and His461 which are found between two conserved FRAP and NPNL boxes.[31] Because FRAP and NPNL boxes are highly conserved, their name and sequence is denoted by one letter amino acid abbreviations. HemR has the capacity to recognize heme, hemoglobin, myoglobin, hemopexin, haptoglobin-hemoglobin, and heme albumin complexes.[31] BhuR is the outer membrane heme receptor in *Bordetella pertussis* and *Bordetella bronchiseptica.*[32] BhuR is very similar to HemR in that it recognizes heme, hemoglobin, haptoglobin-hemoglobin, and heme-albumin.[32] BhuR has been found to be a necessary element of heme uptake,

because upon mutation these species of *Bordetella* were no longer able to utilize these host sources for heme.[32] However BhuR does not contain the two conserved motifs that HemR does, so it may bind to sources of heme differently.

Table 1.1. Comparison of known Gram negative Group II Ton B dependent outer membrane heme receptors, their substrates, and conserved residues and motifs.[30-35]

Bacterium	Receptor	Substrates	Conserved Residues	Conserved Motifs
Y. enterocolitica	HemR	Heme, Hb, Mb, Hx-Heme, Hp-Hb, Heme-HAS	His128 and 461	FRAP, NPNL
P. gingivalis	HmuR	Heme, Hb	His95 and 434	YRAP, NPDL
B. pertussis and B. bronchiseptica	BhuR	Heme, Hb, Hp-Hb, Heme-HAS	None	None
N. meningitidis	HmbR, HpuAB	Hb, Hp-Hb		
P. gingivalis	HmuR	Heme, Hb	His95 and 434	YRAP, NPDL
H. influenzae	HgpA, HgpB, HgpC	Hp-Hb	N/A	N/A
S. dysenteriae	ShuA	Hb	His86 and 428	N/A

In *Neisseria meningitidis* there have been two group II outer membrane receptors identified, HmbR and HpuAB.[33] HmbR is an 89.5 kDa Ton B dependent outer membrane receptor.[33] HpuAB is composed of HpuB, a Ton B dependent receptor and HpuA, a lipoprotein.[33] It has been shown that these receptors are necessary in order to obtain hemoglobin and hemoglobin-haptoglobin from the host environment.[33]

HmuR is the outer membrane heme receptor in *Porphyromonas gingivalis*.[34] HmuR is involved in the uptake of heme and hemoglobin and it works with HmuY which is a heme binding lipoprotein.[34] It is thought to bind through His95 and His434 residues.[35] It is homologous to HemR, ShuA in *Shigella dysenteriae*, and FepA and BtuB in *E. coli*.[34]

In *H. influenzae* strain HI689 there were three hemoglobin, hemoglobin-haptoglobin receptors that were discovered that were named HgpA, HgpB, and HgpC.[36] It was found that any of these three receptors could be used in order to sustain the growth of the organism.[36]

The group II outer membrane receptor in *S. dysenteriae* is ShuA and this appears to use oxidized Hb as a substrate.[37] It has been suggested that the residues His86 and Arg43 depicted in Figure 1.11 shift to bind heme.[37] His86 and His328 were shown to be essential for substrate recognition, heme coordination, and transfer.[37]

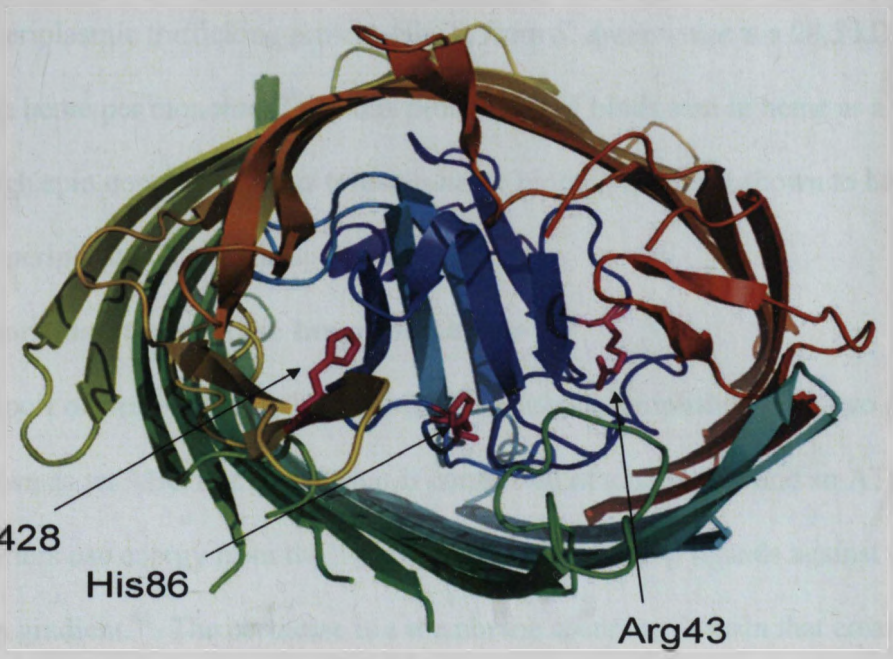

Figure 1.11. Heme binding residues of ShuA from *S. dysenteriae*. Shown above is a cartoon representation of an overhead view down the Ton B dependent β barrel outer membrane heme receptor, ShuA. [18] The residues in pink are integral to the binding of heme.[37]

Iron Transportation in the Periplasm

Once in the periplasmic space heme is bound to a transport protein, which is mechanistically proposed to bring heme to an ABC transporter in the inner membrane.[38]

These proteins are found to have 30-90% sequence homology.[38] Heme is bound in the cleft between the two subdomains of the transport protein, and this cleft is proposed to change conformationally in order to interact with the ABC transporter.[39]

The periplasmic trafficking protein, PhuT, from *P. aeruginosa* is a 33 kDa protein that binds heme with a dissociation constant of 10^{-9}.[39] Interestingly a tyrosine residue has been shown to coordinate heme in this protein instead of the commonly observed coordination of heme via a histidine residue.[39] Tyr71 has been demonstrated to bind heme in its five coordinate high spin configuration in PhuT.[39]

The periplasmic trafficking protein, ShuT, from *S. dysenteriae* is a 28.5 kDa protein that binds one heme per monomer.[40] In this protein Tyr67 binds iron in heme as a five coordinate high spin complex.[40] This tyrosine-heme binding has been shown to be highly conserved in periplasmic heme transporters.[39]

Iron Transportation through the Inner Membrane

Transport of heme through the inner membrane is accomplished via a two protein complex known as an ABC transporter that is comprised of a permease and an ATPase. ABC transporters use energy from the hydrolysis of ATP to pump ligands against a concentration gradient.[41] The permease is a membrane spanning domain that creates a protein-protein interaction with the periplasmic binding protein in order to lower its affinity for heme, thus allowing it to be transported through the inner membrane. The ATPase functions to catalyze the hydrolysis of ATP in order to derive the energy to transport heme into the cytoplasm. ABC transporters have also been shown to be involved in nutrient uptake, osmotic regulation, toxin excretion, and multidrug efflux.[41]

In *S. dysenteriae* transport across the inner membrane was studied in a liposome structure.[42] In this system it was discovered that the periplasmic transport protein ShuT passes heme off to ShuU of the ShuUV complex, where ShuU is the permease and ShuV is the ATPase.[42] It was demonstrated that His252 and His262 of ShuU were necessary in order to release heme from ShuT and deliver it through the inner membrane to the cytoplasmic trafficking protein ShuS.[42]

Transport across the inner membrane in *P. aeruginosa* is performed by the PhuUV complex, where PhuU is the permease and PhuV is the ATPase. There is also a protein that is transcribed directly downfield of the PhuU and PhuV proteins denoted PhuW whose function is not known currently. It was found that this protein shares 30% sequence identity to ChaN in *Campylobacter jejuni*.[8, 43] ChaN consists of a large parallel β sheet with flanking α helices.[43] ChaN forms a dimer like structure that binds two heme groups in a pocket that is formed between two monomers.[43] It was found in ChaN that Tyr148 coordinates the binding of the iron in heme.[43] ChaN is thought to be a lipoprotein associated with the outer membrane functioning to interact with ChaR, an outer membrane receptor in *C. jejuni*.[43]

Iron Transportation and Degradation in the Cytoplasm

Once heme has been transported into the cytoplasm of the Gram negative organism, it could be transferred to a cytoplasmic binding protein or be directly degraded by a heme oxygenase. Figure 1.12 shows the process that the heme oxygenase uses to degrade heme into iron(II), one molecule of carbon monoxide, and biliverdin. Heme oxygenases (HO) function to bind heme at a specific position in the pocket of the protein to form a heme-HO complex with histidine as the coordinating heme-iron ligand.[44] What distinguishes heme

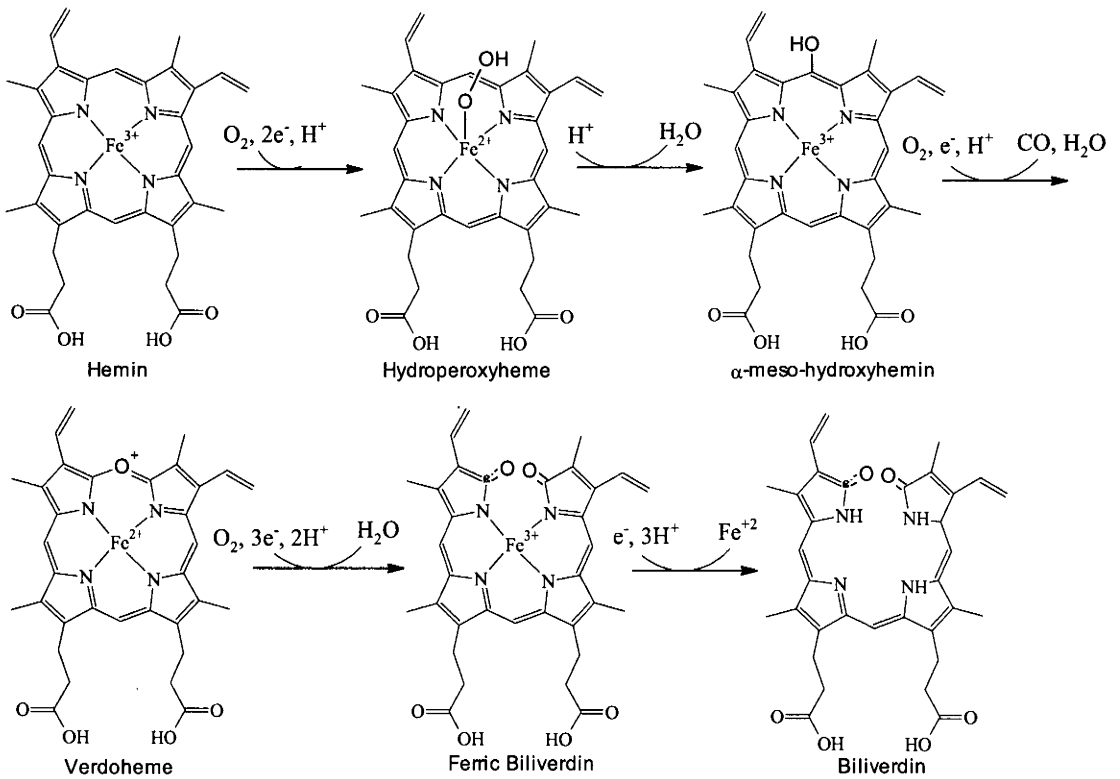

Figure 1.12. Regiospecific degradation of heme by heme oxygenase. Depicted is the regiospecific degradation of heme by heme oxygenase in three successive oxygenase reactions. The first oxygenation step of this reaction involves the addition of two electrons from NADPH-cytochrome P450 reductase and molecular oxygen reduces ferric iron to ferrous iron through the creation of a hydroperoxyheme complex.[45] The second oxygenation reaction involves the protonation of the hydroperoxygen complex to form water and α-meso-hydroxyhemin.[46] One electron from NADPH-cytochrome P450 reductase as well as molecular oxygen reduces iron (III) to iron (II) or verdoheme releasing one molecule of carbon monoxide and water.[46] In the third oxygenation reaction, three electrons from NADPH-cytochrome P450 reductase and molecular oxygen oxidize iron and cause the ring structure to cleave at the meso position creating ferric biliverdin and water.[46a] This has been determined to be the rate-limiting step of the heme oxygenase reaction.[46a] One additional electron from NADPH-cytochrome P450 reductase is added to the reaction and iron(II) is released creating biliverdin.[46a] Biliverdin is an antioxidant that allows for protection against oxidative stress within the cell.[46a]

oxygenases from other heme degrading compounds is their regioselective hydroxylation of an α-meso carbon on the protoporphyrin IX ring.[45] There have been three heme oxygenases that have been identified in bacteria to date: pa-HO from *P. aeruginosa*, nm-

HO from *N. meningitidis*, and cd-HO from *Corynebacterium diphtheriae*. Heme oxygenase activity has not been detected in *S. dysenteriae*.

ShuS is the cytoplasmic heme transport protein from *S. dysenteriae*. It was found to be sixty percent homologous with HemS, and it has a dissociation constant for heme of 10^{-7} molar.[42] ShuS has been found to function as a heme storage protein as well as a DNA binding protein.[42] This DNA binding is thought to protect the organism against heme-induced oxidative damage.[42]

Table 1.2 shows a list of some Gram negative bacterial cytoplasmic binding proteins. HemS from *Y. enterocolitica* has been shown to bind and then release heme, so it has been proposed to exist as a heme transporter in the cytoplasm.[47] His196 has been shown to coordinate to the iron in the heme bound complex, while a distal Arg102

Table 1.2. Gram negative cytoplasmic binding proteins.

Bacterium	Cytoplasmic Binding Protein
Y. enterocolitica	HemS
S. dysenteriae	ShuS
E. coli	ChuS
Y. pestis	HmuS
P. aeruginosa	PhuS

stabilizes this complex.[47] ChuS is a cytoplasmic protein in *E. coli* that shares ninety-eight percent sequence homology with ShuS, but was claimed to be a heme oxygenase by Suits *et. al.*.[48] The claim was made that ChuS was a heme oxygenase because in the presence of ascorbic acid the protein did oxygen dependent heme degradation, creating verdoheme and

carbon monoxide.[48] However heme oxygenases cleave regiospecifically and ChuS was not shown to cleave in this manner, so the protein more than likely functions as a cytoplasmic transporter for heme or degrades heme using a mechanism different from a traditional heme oxygenase.

HmuS is the cytoplasmic heme binding protein in *Y. pestis*, that was initially thought to be a heme oxygenase as well.[49] Inactivation of this protein showed that mutants were still able to use heme and hemoproteins as an iron source, so the proposed function is that HmuS is involved in heme storage and/or chaperoning.[49]

PhuS is a 39 kDa cytoplasmic heme transportation protein from *P. aeruginosa*. PhuS has been shown to function to pass heme in the cytoplasm to a heme oxygenase.[50] The protein has been demonstrated to bind one heme per monomer with alternate His ligands at positions 209 and 212.[50] When PhuS was placed in solution containing ascorbic acid, it was not observed to exhibit heme oxygenase activity, because heme ring opening activity occurred at a very slow rate.[51] The crystal structure of PhuS remains unsolved, but it is highly homologous with ChuS.[50]

Iron Acquisition of *Pseudomonas aeruginosa*

P. aeruginosa is an opportunistic pathogen that has become a large problem for immunocompromised individuals, particularly those with cystic fibrosis. *P. aeruginosa* is one of the largest inhabitants of the mucosa that lines the lungs of these patients, where it forms biofilms.[52] Ultimately it, amongst other bacterial and fungal inhabitants, is the cause of death in these patients whose chronic infection eventually becomes multi-drug resistant and hard to treat due to these biofilm formations.[52] Because *P. aeruginosa* is iron-limited there could be the potential to disrupt its iron acquisition system in order to help combat the

infection. Therefore it is important to know how this bacterium obtains its iron from the host environment.

There are two ways in which *P. aeruginosa* can obtain iron from its environment. The first way is through a receptor in the bacterium that recognizes host heme proteins, and the second is through a secreted complex. The secreted complexes that *P. aeruginosa* uses are siderophores and hemophores.

Figure 1.13 depicts a scheme of the direct host uptake of heme from *P. aeruginosa*. Heme is transported into the periplasmic space via the PhuR receptor that is TonB dependent. The energy for this process is derived through a proton gradient coupled to the

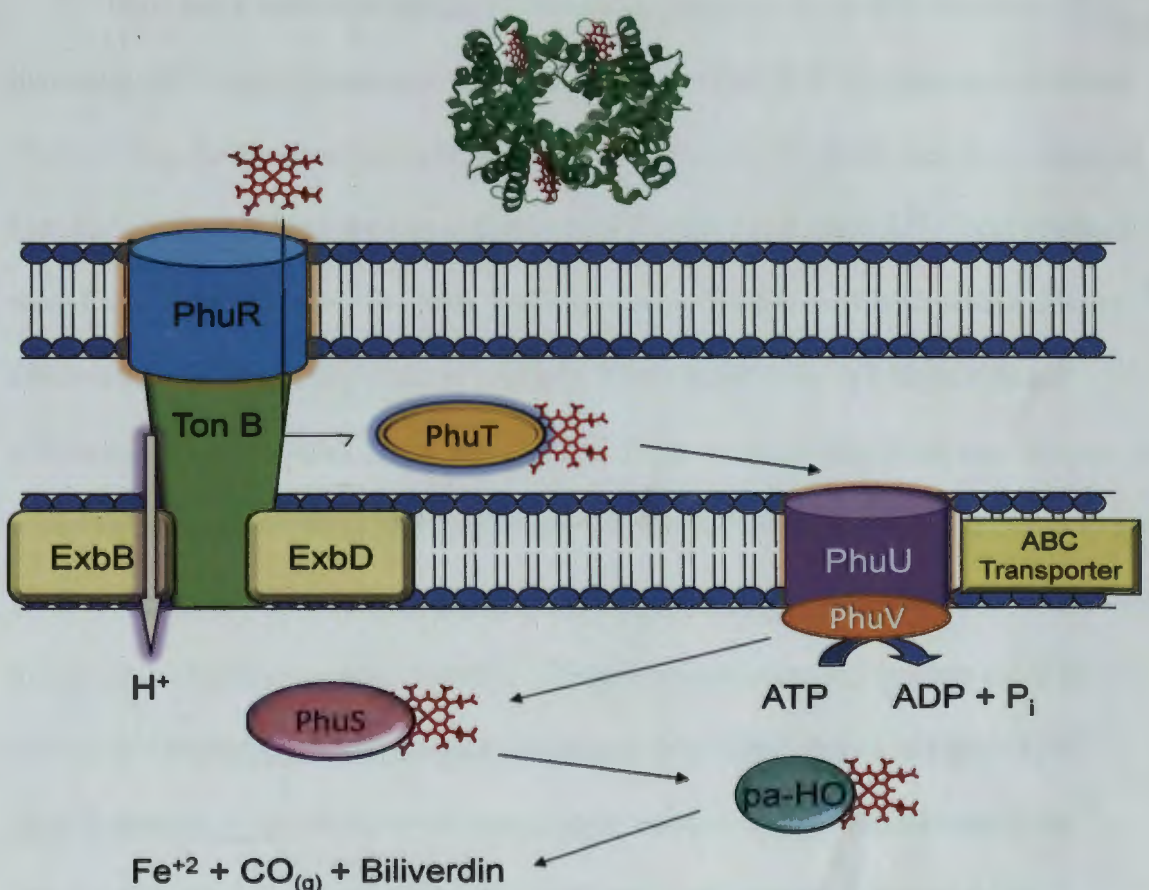

Figure 1.13. Cartoon representation of the *Phu* system of *P. aeruginosa*. The green protein is a cartoon representation of hemoglobin, and the red structure is heme.[53]

inner membrane by the ExbB and ExbD proteins. Heme is then passed off to PhuT, a periplasmic heme trafficking protein that transports heme to the ABC transporter complex, PhuUV. PhuU is a permease that spans the inner membrane and allows passing of heme from PhuT by creating a protein-protein interaction. PhuV is an ATPase that catalyzes the hydrolysis of ATP to yield ADP and an inorganic phosphate. The free energy of this reaction provides the energy to bring heme to the cytoplasmic space. Once inside of the cytoplasm, heme is bound to PhuS, a cytoplasmic trafficking protein that transfers heme to a heme oxygenase so that it can be degraded into Fe(II), carbon monoxide, and biliverdin.

PhuS

PhuS has a molecular weight of 39 kDa and it shares 39 to 98 % sequence homology with other cytoplasmic trafficking proteins: HemS of *Yersinia enterocolitica*, ShuS of *Shigella dysenteriae*, and ChuS of *Escherichia coli*.[50] PhuS uses two conserved histidine residues to bind the iron center in heme, His209 and His212.[50] These residues were found to be necessary for heme binding upon performance of mutagenesis studies. [50] Observed histidine binding sites are similarly found in the other cytoplasmic heme trafficking proteins: HemS, ShuS, and ChuS.[50] From studies where PhuS was knocked out it was determined that PhuS was a necessary element for effective heme utilization to occur in *P. aeruginosa*.[54] The activity of PhuS as a heme oxygenase was tested and it was found to not exhibit heme oxygenase activity.[55] The crystal structure of PhuS has yet to be solved, so a homology model has been developed from ChuS shown in Figure 1.14.[50] PhuS is located on the *Phu* (*Pseudomonas* heme uptake) operon which contains the proteins that comprise *P. aeruginosa*'s direct heme uptake system (Figure 1.15).

Figure 1.14. Homology structure of PhuS derived from ChuS in *Eschericia coli*.[50, 56]

Figure 1.15. Illustration of the *Phu* operon from *P. aeruginosa*. The above cartoon is adapted from Tong *et al.*[29] PhuR is the receptor for the direct uptake of heme. PhuS is a cytoplasmic heme trafficking protein, PhuT is a periplasmic heme trafficking protein. PhuU and PhuV make up the PhuUV complex which is an ABC transporter. PhuU is the permease and PhuV is the ATPase which catalyzes the hydrolysis of ATP in order to bring heme in through the inner membrane. The function of PhuW still remains unknown. Fur is the ferric uptake regulator which functions to regulate the transcription of the Phu genes depending on if iron is deplete or replete in the bacterial system.

PhuS binds heme in two sequential steps to yield distinct complexes that are known as holo PhuS and half-holo PhuS (Figure 1.16).[50] Holo PhuS is heme that is bound to the protein in a 1:1 ratio. Half-holo PhuS is heme that is bound to the protein in a 1 heme:2 protein ratio. For half-holo PhuS the dissociation constant is 0.10 ± 0.01 μM and for holo PhuS the dissociation constant is 0.40 ± 0.02 μM.[50]

P. aeruginosa uses several methods to obtain iron from its host environment. After iron is taken into the system through the outer membrane, the Has pathway and direct heme uptake pathways are thought to be redundant. The Has and direct systems are thought to use the same periplasmic binding protein and ABC transporter.[5] Therefore more work can be done to better understand the internalization of iron in the periplasmic and cytoplasmic space so that the uptake of host iron can be stopped. Since *P. aeruginosa* is an iron-limited bacterium, understanding its iron uptake pathways could help lead to more effective treatment of infection in the host environment.

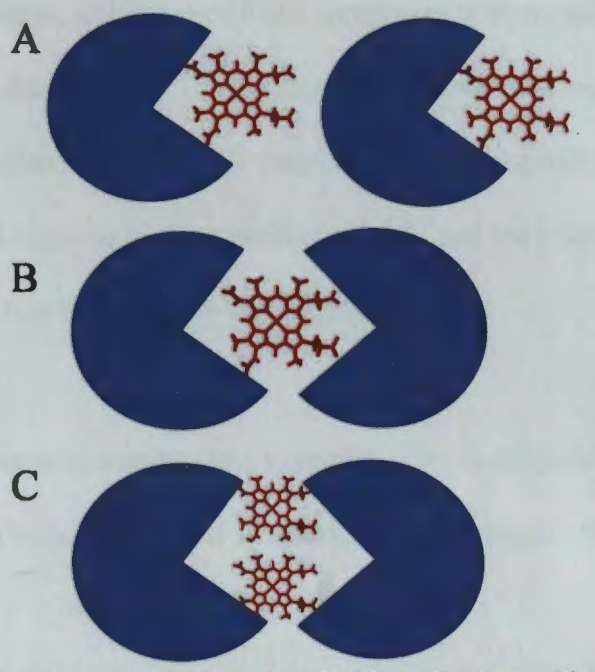

Figure 1.16. Cartoon illustrations of the molecularities of holo and half-holo PhuS. A and C) Cartoon illustrations of the possible molecularities of holo PhuS. B) Cartoon representation of half-holo PhuS. The red structure represents heme, while the blue circle represents PhuS.

Goals of this Study

The relationship between structure and function of iron transport proteins is being pieced together by a combination of efforts from the scientific community. These proteins

are able to do directed heme transfer through specific protein-protein interactions that allow heme to be transferred from a higher affinity protein to a lower affinity protein. Understanding the iron acquisition pathways of bacteria is important because almost all bacteria require iron in order to survive. Therefore these pathways can be a potential target to pursue for treatment of bacterial infections.

The broad goal of this research is to investigate the feasibility of inhibiting heme uptake and/or trafficking by Gram negative pathogens. Hence, the results of this work could support the development of new strategies for clinical treatments against their infections. Thermodynamic stabilities of PhuS complexes with metalloporphyrins that mimic heme have been determined. The non-bonding interactions between porphyrin ligands and PhuS were also of interest. Looking into these non-bonding interactions could show us if metal-ligand bonding of the metalloporphyrin and the protein is necessary in order for the protein to function in heme trafficking.

References

1. Bruyneel, B.; vande Woestyne, M.; Verstraete, W., Lactic acid bacteria: Micro-organisms able to grow in the absence of available iron and copper. *Biotechnology Letters* **1989,** *11* (6), 401-406.

2. Bartholomew, J. W.; Mittwer, T., The Gram Stain. *Bacteriol Rev.* **1952,** *16*, 1-29.

3. Kaplan, C. D.; Kaplan, J., Iron Acquisition and Transcriptional Regulation. *Chemical Reviews* **2009,** *109* (10), 4536-4552.

4. Storz, G.; Imlayt, J. A., Oxidative Stress. *Current Opinion in Microbiology* **1999,** *2* (2), 188-194.

5. Wandersman, C.; Delepelaire, P., Bacterial Iron Sources: From Siderophores to Hemophores. *Annual Review of Microbiology* **2004,** *58* (1), 611-647.

6. Shikama, K.; Matsuoka, A., Human haemoglobin. *European Journal of Biochemistry* **2003,** *270* (20), 4041-4051.

7. Bacarella, A. L.; Grunwald, E.; Marshall, H. P.; Purlee, E. L., The Potentiometric Measurement of Acid Dissociation Constants and pH in the System Methanol-Water: pKa Values for Carboxylic Acids and Anilinium Ions. *The Journal of Organic Chemistry* **1955,** *20* (6), 747-762.

8. Tong, Y.; Guo, M., Bacterial heme-transport proteins and their heme-coordination modes. *Archives of Biochemistry and Biophysics* **2009,** *481* (1), 1-15.

9. Reichlin, M., Hemoglobin and Myoglobin in their Reactions with Ligands. *Science* **1972,** *178* (4058), 296.

10. Weinberg, E. D., Iron availability and infection. *Biochimica et Biophysica Acta (BBA) - General Subjects* **2009,** *1790* (7), 600-605.

11. Czernoszewicz, R. S., Theoretical and Physical Characterization. In *The Porphyrin Handbook*, Kadish, Ed. Academic Press: London, 2000; Vol. 7.

12. Nemeth, E.; Tuttle, M. S.; Powelson, J.; Vaughn, M. B.; Donovan, A.; Ward, D. M.; Ganz, T.; Kaplan, J., Hepcidin Regulates Cellular Iron Efflux by Binding to Ferroportin and Inducing Its Internalization. *Science* **2004,** *306* (5704), 2090-2093.

13. Wandersman, C.; Stojiljkovic, I., Bacterial heme sources: the role of heme, hemoprotein receptors and hemophores. *Current Opinion in Microbiology* **2000,** *3* (2), 215-220.

14. Ferguson, A. D.; Deisenhofer, J., TonB-dependent receptors--structural perspectives. *Biochimica et Biophysica Acta (BBA) - Biomembranes* **2002,** *1565* (2), 318-332.

15. Wiener, M. C., TonB-dependent outer membrane transport: going for Baroque? *Current Opinion in Structural Biology* **2005,** *15* (4), 394-400.

16. Neilands, J. B., Siderophores: Structure and Function of Microbial Iron Transport Compounds. *Journal of Biological Chemistry* **1995,** *270* (45), 26723-26726.

17. Krewulak, K. D.; Vogel, H. J., Structural biology of bacterial iron uptake. *Biochimica et Biophysica Acta (BBA) - Biomembranes* **2008,** *1778* (9), 1781-1804.

18. Cobessi, D.; Celia, H.; Folschweiller, N.; Schalk, I. J.; Abdallah, M. A.; Pattus, F., The Crystal Structure of the Pyoverdine Outer Membrane Receptor FpvA from Pseudomonas aeruginosa at 3.6 A Resolution. *Journal of Molecular Biology* **2005,** *347* (1), 121-134.

19. Caillet-Saguy, C.; Delepierre, M.; Lecroisey, A.; Bertini, I.; Piccioli, M.; Turano, P., Direct-Detected 13C NMR to Investigate the Iron(III) Hemophore HasA. *Journal of the American Chemical Society* **2005,** *128* (1), 150-158.

20. Letoffe, S.; Ghigo, J. M.; Wandersman, C., Secretion of the Serratia marcescens HasA protein by an ABC transporter. *J. Bacteriol.* **1994,** *176* (17), 5372-5377.

21. Delepelaire, P.; Wandersman, C., The SecB chaperone is involved in the secretion of the Serratia marcescens HasA protein through an ABC transporter. *EMBO J* **1998,** *17* (4), 936-944.

22. Krieg, S.; Huché, F.; Diederichs, K.; Izadi-Pruneyre, N.; Lecroisey, A.; Wandersman, C.; Delepelaire, P.; Welte, W., Heme uptake across the outer membrane as

revealed by crystal structures of the receptor–hemophore complex. *Proceedings of the National Academy of Sciences* **2009,** *106* (4), 1045-1050.

23. Arnoux, P.; Haser, R.; Izadi, N.; Lecroisey, A.; Delepierre, M.; Wandersman, C.; Czjzek, M., The crystal structure of HasA, a hemophore secreted by Serratia marcescens. *Nature Structural Biology* **1999,** *6* (6), 516.

24. Cescau, S.; Cwerman, H.; Létoffé, S.; Delepelaire, P.; Wandersman, C.; Biville, F., Heme acquisition by hemophores. *BioMetals* **2007,** *20* (3), 603-613.

25. Letoffe, S.; Delepelaire, P.; Wandersman, C., Free and Hemophore-Bound Heme Acquisitions through the Outer Membrane Receptor HasR Have Different Requirements for the TonB-ExbB-ExbD Complex. *J. Bacteriol.* **2004,** *186* (13), 4067-4074.

26. Létoffé, S.; Deniau, C.; Wolff, N.; Dassa, E.; Delepelaire, P.; Lecroisey, A.; Wandersman, C., Haemophore-mediated bacterial haem transport: evidence for a common or overlapping site for haem-free and haem-loaded haemophore on its specific outer membrane receptor. *Molecular Microbiology* **2001,** *41* (2), 439-450.

27. Hanson, M. S.; Pelzel, S. E.; Latimer, J.; Muller-Eberhard, U.; Hansen, E. J., Identification of a genetic locus of Haemophilus influenzae type b necessary for the binding and utilization of heme bound to human hemopexin. *Proceedings of the National Academy of Sciences of the United States of America* **1992,** *89* (5), 1973-1977.

28. Coy, M.; Neilands, J. B., Structural dynamics and functional domains of the Fur protein. *Biochemistry* **1991,** *30* (33), 8201-8210.

29. Tong, Y.; Guo, M., Cloning and characterization of a novel periplasmic heme-transport protein from the human pathogen Pseudomonas aeruginosa. *Journal of Biological Inorganic Chemistry* **2007,** *12* (6), 735-750.

30. Stojiljkovic, I.; Hantke, K., Functional domains of the Escherichia coli ferric uptake regulator protein (Fur). *Molecular and General Genetics MGG* **1995,** *247* (2), 199-205.

31. Bracken, C. S.; Baer, M. T.; Abdur-Rashid, A.; Helms, W.; Stojiljkovic, I., Use of Heme-Protein Complexes by the Yersinia enterocolitica HemR Receptor: Histidine Residues Are Essential for Receptor Function. *J. Bacteriol.* **1999,** *181* (19), 6063-6072.

32. Vanderpool, C. K.; Armstrong, S. K., The Bordetella bhu Locus Is Required for Heme Iron Utilization. *J. Bacteriol.* **2001,** *183* (14), 4278-4287.

33. Lewis, L. A.; Sung, M.-H.; Gipson, M.; Hartman, K.; Dyer, D. W., Transport of Intact Porphyrin by HpuAB, the Hemoglobin-Haptoglobin Utilization System of Neisseria meningitidis. *J. Bacteriol.* **1998,** *180* (22), 6043-6047.

34. Simpson, W.; Olczak, T.; Genco, C. A., Characterization and Expression of HmuR, a TonB-Dependent Hemoglobin Receptor of Porphyromonas gingivalis. *J. Bacteriol.* **2000,** *182* (20), 5737-5748.

35. Liu, X.; Olczak, T.; Guo, H.-C.; Dixon, D. W.; Genco, C. A., Identification of Amino Acid Residues Involved in Heme Binding and Hemoprotein Utilization in the Porphyromonas gingivalis Heme Receptor HmuR. *Infect. Immun.* **2006,** *74* (2), 1222-1232.

36. Jin, H.; Ren, Z.; Pozsgay, J.; Elkins, C.; Whitby, P.; Morton, D.; Stull, T., Cloning of a DNA fragment encoding a heme-repressible hemoglobin- binding outer membrane protein from Haemophilus influenzae. *Infect. Immun.* **1996,** *64* (8), 3134-3141.

37. Burkhard, K. A.; Wilks, A., Characterization of the Outer Membrane Receptor ShuA from the Heme Uptake System of Shigella dysenteriae. *Journal of Biological Chemistry* **2007,** *282* (20), 15126-15136.

38. Stojiljkovic, I.; Perkins-Balding, D., Processing of Heme and Heme-Containing Proteins by Bacteria. *DNA & Cell Biology* **2002,** *21* (4), 281-295.

39. Ho, W. W.; Li, H.; Eakanunkul, S.; Tong, Y.; Wilks, A.; Guo, M.; Poulos, T. L., Holo- and Apo-bound Structures of Bacterial Periplasmic Heme-binding Proteins. *Journal of Biological Chemistry* **2007,** *282* (49), 35796-35802.

40. Eakanunkul, S.; Lukat-Rodgers, G. S.; Sumithran, S.; Ghosh, A.; Rodgers, K. R.; Dawson, J. H.; Wilks, A., Characterization of the Periplasmic Heme-Binding Protein ShuT from the Heme Uptake System of Shigella dysenteriae†. *Biochemistry* **2005,** *44* (39), 13179-13191.

41. Higgins, C. F.; Linton, K. J., The ATP switch model for ABC transporters. *Nat. Struct. Mol. Biol.* **2004,** *11*, 918-926.

42. Wilks, A., The ShuS Protein of Shigella dysenteriae Is a Heme-Sequestering Protein That Also Binds DNA. *Archives of Biochemistry and Biophysics* **2001,** *387* (1), 137-142.

43. Chan, A. C. K.; Lelj-Garolla, B.; I. Rosell, F.; Pedersen, K. A.; Mauk, A. G.; Murphy, M. E. P., Cofacial Heme Binding is Linked to Dimerization by a Bacterial Heme Transport Protein. *Journal of Molecular Biology* **2006,** *362* (5), 1108-1119.

44. Kikuchi, G.; Yoshida, T.; Noguchi, M., Heme oxygenase and heme degradation. *Biochemical and Biophysical Research Communications* **2005,** *338* (1), 558-567.

45. Matsui, T.; Unno, M.; Ikeda-Saito, M., Heme oxygenase reveals its strategy for catalyzing three successive oxygenation reactions. *Acc. Chem. Res.* **2010,** *43*, 240-247.

46. (a) Matsui, T.; Unno, M.; Ikeda-Saito, M., Heme oxygenase reveals its strategy for catalyzing three successive oxygenation reactions. *Acc. Chem. Res.* **2010,** *43* (Copyright

(C) 2010 American Chemical Society (ACS). All Rights Reserved.), 240-247; (b) Gohya, T.; Sato, M.; Zhang, X.; Migita, C. T., Variation of the oxidation state of verdoheme in the heme oxygenase reaction. *Biochemical and Biophysical Research Communications* **2008,** *376* (2), 293-298.

47. Schneider, S.; Sharp, K. H.; Barker, P. D.; Paoli, M., An Induced Fit Conformational Change Underlies the Binding Mechanism of the Heme Transport Proteobacteria-Protein HemS. *Journal of Biological Chemistry* **2006,** *281* (43), 32606-32610.

48. Suits, M. D. L.; Pal, G. P.; Nakatsu, K.; Matte, A.; Cygler, M.; Jia, Z., Identification of an Escherichia coli O157:H7 heme oxygenase with tandem functional repeats. *Proc. Natl. Acad. Sci. U. S. A.* **2005,** *102*, 16955-16960.

49. Thompson, J. M.; Jones, H. A.; Perry, R. D., Molecular Characterization of the Hemin Uptake Locus (hmu) from Yersinia pestis and Analysis of hmu Mutants for Hemin and Hemoprotein Utilization. *Infect. Immun.* **1999,** *67* (8), 3879-3892.

50. Block, D. R.; Lukat-Rodgers, G. S.; Rodgers, K. R.; Wilks, A.; Bhakta, M. N.; Lansky, I. B., Identification of Two Heme-Binding Sites in the Cytoplasmic Heme-Trafficking Protein PhuS from Pseudomonas aeruginosa and Their Relevance to Function. *Biochemistry* **2007,** *46* (50), 14391-14402.

51. Friedman, J.; Meharenna, Y. T.; Wilks, A.; Poulos, T. L., Diatomic Ligand Discrimination by the Heme Oxygenases from Neisseria meningitidis and Pseudomonas aeruginosa. *Journal of Biological Chemistry* **2007,** *282* (2), 1066-1071.

52. Lamont, I.; Konings, A.; Reid, D., Iron acquisition by Pseudomonas aeruginosa in the lungs of patients with cystic fibrosis. *BioMetals* **2009,** *22* (1), 53-60.

53. Kovalevsky, A. Y.; Chatake, T.; Shibayama, N.; Park, S.-Y.; Ishikawa, T.; Mustyakimov, M.; Fisher, Z.; Langan, P.; Morimoto, Y., Direct Determination of Protonation States of Histidine Residues in a 2 Å Neutron Structure of Deoxy-Human Normal Adult Hemoglobin and Implications for the Bohr Effect. *Journal of Molecular Biology* **2010,** *398* (2), 276-291.

54. Kaur, A. P.; Lansky, I. B.; Wilks, A., The Role of the Cytoplasmic Heme-binding Protein (PhuS) of Pseudomonas aeruginosa in Intracellular Heme Trafficking and Iron Homeostasis. *J. Biol. Chem.* **2009,** *284*, 56-66.

55. Lansky, I. B.; Lukat-Rodgers, G. S.; Block, D.; Rodgers, K. R.; Ratliff, M.; Wilks, A., The Cytoplasmic Heme-binding Protein (PhuS) from the Heme Uptake System of Pseudomonas aeruginosa Is an Intracellular Heme-trafficking Protein to the δ-Regioselective Heme Oxygenase. *Journal of Biological Chemistry* **2006,** *281* (19), 13652-13662.

56. Block, D. R. Biophysical Studies of Heme Assimilation Proteins from Pathogenic Bacteria. NDSU, Fargo, ND, 2009.

CHAPTER 2: MATERIALS AND METHODS

Introduction

This chapter describes the materials, the experimental methods, and the data analysis methods that have been applied to this investigation of the thermodynamics of metalloporphyrin binding to PhuS. A discussion of how PhuS was produced begins the chapter, followed by the synthesis of the metalloporphyrins used in the spectrophotometric titrations of PhuS. Next a detailed description of the titration experiments, along with a description of the data analysis for determining the binding constants is provided.

The pET Plasmid as an Expression Vector in *E. coli*

The pET plasmid has been designed for use as an expression vector, commonly in the BL21(DE3) strain of *Escherichia coli*. A gene sequence that encodes for a protein of interest that has been incorporated into the pET plasmid can exploit the bacterial machinery in order to become over produced within the bacterial cell. Protein from diverse species can therefore be synthesized in less time through this over expression method than by isolation and purification of the protein from its native organism.

The pET plasmid comprises 5.4 thousand base pairs, and contains genes that allow it to act as a vector for the over-expression of proteins. In order to use the pET plasmid as an expression vector, the gene sequence encoding the protein of interest must be integrated into the plasmid at the polylinker region.[1] Then the plasmid is transformed into the BL21(DE3) *E. coli* cell. The plasmid contains an origin of replication (ori) site, where replication of the plasmid begins. The plasmid also contains the amp^R gene which encodes for a β-lactamase that imparts resistance to the antibiotic ampicillin. When the bacterial culture is grown in presence of ampicillin, only the *E. coli* cells containing the pET plasmid

with the *amp*^{R} gene have a survival advantage. Therefore the growth medium is selective for the *E. coli* cells containing the pET plasmid. The plasmid also contains the PT7 transcription promoter, which is derived from the T7 bacteriophage.[1] Assimilation of this promoter into the plasmid exploits phage genetics which function to massively produce viral DNA in order to propagate the phage.[1] The plasmid contains the *lac* promoter, which contains an operator site that forms a tight complex with the *lac* repressor, LacI, in the absence of lactose. This protein-DNA complex prevents RNA polymerase from advancing to the gene(s) under the regulatory control of the promoter. Thus, transcription of those genes is repressed. Lactose binds strongly to LacI and acts as an allosteric effector that drastically diminishes the stability of the LacI-DNA complex. Thus *lac*O, the *lac* operator, will be bound by LacI unless lactose is present.[1] This will allow the experiment to be controlled so that expression of the protein can be started once the culture reaches a significant density of bacterial cells. As long as T7 RNA polymerase is present and the lactose operator encoded on the plasmid are being transcribed, this promoter will act to over-express the protein encoded within the plasmid.[1]

A culture is initiated by inoculating a solution containing media that supports bacterial growth with the bacteria containing the plasmid. Once the bacterial culture has reached an optical density of 0.6 at 600 nm, it is induced by addition of isopropyl β-D-1-thiogalactopyranoside (IPTG). The addition of this lactose analogue causes LacI to stop dissociate from the DNA, thereby derepressing the *lac* operator. This activates the T7 promoter, facilitating transcription of the gene(s) under its control and over-expresses the respective proteins.[1] Typically this culture is allowed to continue growth for an additional

one to two hours before the cells are harvested and lysed to release the protein. The protein can then be isolated and purified using methods appropriate for the system at hand.

Preparation of the pET21 BL21(DE3) *E. coli* Cells

The pET21 plasmid containing the PhuS sequence (pET21PhuS) was supplied by the Wilks group in the Department of Pharmaceutical Science at the University of Maryland, Baltimore County. Competent DH5α cells purchased from Invitrogen were transformed with pET21PhuS via the protocol contained in the kit. The plasmid was then isolated using a Promega Wizard Miniprep Purification kit. The isolated pET21PhuS plasmid was introduced into competent BL21DE3 *E. coli* cells by following the protocol from the Novagen singles kit. A frozen permanent of the transformed BL21DE3 *E. coli* cells in lysogeny broth (LB) media in their saturation growth phase was made in 25 mM Tris-HCl pH = 8.0, 8% glycerol and stored at − 80° C. The frozen permanent was then used to inoculate 100 mL subcultures which in turn were used to inoculate 1 L LB cultures for over-expression of PhuS.

Preparation of PhuS

PhuS was isolated and purified by a modification of the previously published procedure.[2] Modifications included removal of Triton-X from all buffers and inclusion of 1-2 column volumes of 1 mM phenylmethylsulfonyl fluoride (PMSF) and 10 mM benzamidine before addition of PhuS to the HiTrap™ Q Sepharose™ anion exchange column. Triton-X was removed from the procedure because it is a surfactant that solubilizes membrane proteins, and the protein of interest is not membrane-bound. PMSF and benzamidine were included in the procedure because they are protease inhibitors which act to inhibit degradation of the protein by proteases. Also the volume of the salt gradient

on the ion exchange column was increased from 10 column volumes to 20 column volumes to improve separation of PhuS from other proteins in the extract.

PhuS was eluted from the HiTrap™ Q ion exchange column with a linear salt gradient of 20 column volumes ranging from 50-400 mM NaCl. PhuS eluted at 200 mM NaCl. The chromatographic fractions containing PhuS were combined and concentrated to reduce their collective volume to one milliliter for further HPLC purification using a Superdex 200 size exclusion column. Figure 2.1 shows the UV-visible absorbance spectrum of PhuS.

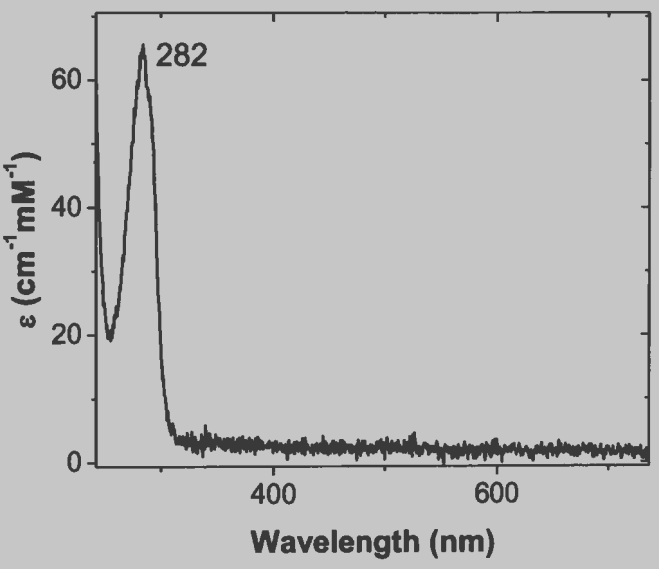

Figure 2.1. Typical UV-visible absorbance spectra of PhuS. PhuS exhibits a characteristic tryptophan absorbance peak at 282 nm.

The concentration of the protein in the sample was determined by the extinction coefficient at 282 nm of 6.3×10^4 $M^{-1} \cdot cm^{-1}$.[2] The protein was then frozen and stored at −80 ° C in 100 µL aliquots of 30 µM PhuS. This protein could then be loaded with heme or other metalloporphyrins for the binding studies described below.

FeTPPS Synthesis

The ligand meso-tetra (4-sulfonatophenyl) porphine dihydrochloride was purchased from Frontier Scientific and metallated with iron to yield FeTPPS via the method described by Herrmann *et al.* (Figure 2.2A).[3] In order to metallate the free porphyrin, an aqueous solution of the free-base porphyrin (50 mg H_2TPPS) was boiled in the presence of a 20 fold excess of granular elemental iron. The iron was first rinsed with 1.0 M HCl in order to remove oxides from its surface. The reaction was monitored via UV-visible spectroscopy until completion which occurred after approximately one hour, as indicated by the disappearance of two Q bands from the visible spectrum. The free H_2TPPS spectrum exhibits four Q bands while the metallated porphyrin exhibits only two. The reaction solution exhibited a color change from dark green (H_4TPPS^{2+}) to a dark purple (FeTPPS). Excess solid metal was removed from the reaction mixture via vacuum filtration, and the volume of the aqueous solution was reduced by rotary evaporation. The metalloporphyrin was applied to a CM52 carboxymethyl cellulose cation exchange column and eluted with aqueous NaCl in order to exchange the hydrogen ions on the sulfonate groups with sodium. A 1:1:1 (v:v:v) ratio of methanol:acetone:water was added to the metalloporphyrin and the volume was reduced by rotary evaporation. The metalloporphyrin was precipitated by adding a twenty-fold excess (v:v) of acetone to the concentrated metalloporphyrin solution. The solid was collected via vacuum filtration and dried under vacuum over night at ambient temperature.

To confirm that the desired product had been obtained (Figure 2.2C), FeTPPS was analyzed via ^1H NMR spectroscopy and compared with spectra available in the literature.[4] These spectra are shown in Figure 2.3. The data show that FeTPPS is a mixture of the

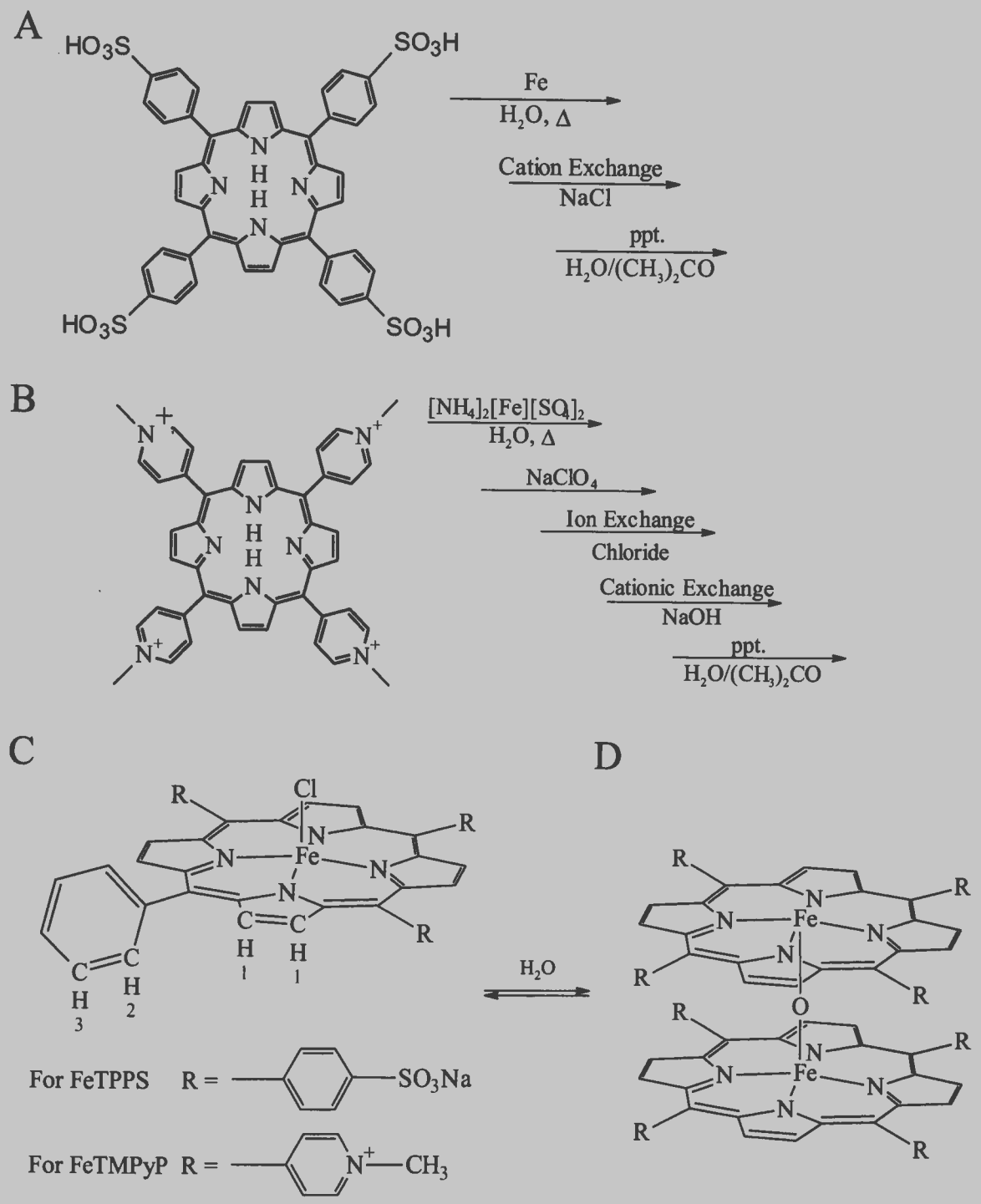

Figure 2.2. Synthesis reactions of FeTPPS and FeTMPyP. (A) Synthesis reaction of FeTPPS (B) Synthesis reaction of FeTMPyP (C) High spin monomeric structure of FeTPPS and FeTMPyP (D) μ-oxo-dimeric structure of FeTPPS and FeTMPyP.

high-spin monomeric and dimeric forms, both of which occur in aqueous solution near neutral pH. FeTPPS has a pK_a of 7.8.[5] Below pH 7.8, the high-spin monomeric complex dominates and above this it will be in its dimeric form.[5]

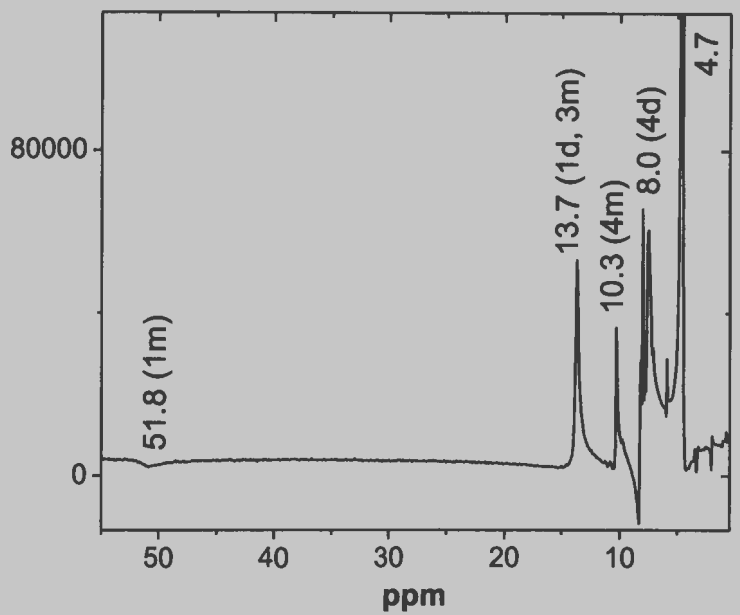

Figure 2.3. Labeled ^{1}H NMR spectra for FeTPPS.[4] In the NMR the numbers listed above the peaks correspond to the labeled hydrogens in Figure 2C. The lowercase letters m and d denote which species the hydrogens are located on: the high spin monomer or the μ-oxo dimer form of the metalloporphyrin respectively. The peak at 4.7 occurs due to HDO present from the solvent D_2O. The frequency of the spectrometer used was 400 mHz. The number of data points recorded was 8,192, with a pulse width of 6.25 μs, and an acquisition time of 34.2 ms. The recovery delay for this experiment was 20 μs and the line broadening factor was 45 Hz.

FeTPPS exhibits a shift at 13.7 ppm that represents the ortho hydrogens from the sodium-sulfonato phenyl ring, as well as the beta pyrrole hydrogens from the μ-oxo dimeric complex. The shifts at 10.3 and 8.0 ppm are due to the meta hydrogens from the sodium-sulfonato phenyl ring of the monomeric and dimeric FeTPPS respectively. FeTPPS also exhibits a broad peak at 51 ppm which is due to the beta pyrrole hydrogens from the monomeric porphyrin ring. The magnetic moment of the paramagnetic iron(III) center of

the monomer is what causes the shift at 51 ppm to be so far downfield from the other shifts of the sulfonato phenyl side chains.

FeTMPyP Synthesis

Meso-5,10,15,20-tetrakis-(4-N-methyl-4-pyridyl)-porphine tetra tosylate (hereinafter abbreviated as H_2TMPyP) was purchased from Frontier Scientific. Iron was inserted in this porphyrin to yield $[FeTMPyP]^{5+}$ and purified via the methods described by Pasternack, *et al.* (Figure 2.2B).[6] In order to metallate H_2TMPyP, 50 mg of the free-base porphyrin were dissolved in 100 mL of water containing a 100-fold excess of ferrous ammonium sulfate. The UV-visible spectrum of this solution was monitored for the disappearance of two Q bands and judged complete after two hours. The spectrum of the unmetallated porphyrin in solution with the metal comprises a Soret band with a maximum at 420 nm and a shoulder at 400 nm. As described by Pasternack *et. al.*, upon metallation of the porphyrin, the main peak shifts to 400 nm with a shoulder at 420 nm.[6] The solution was then cooled and a 100 fold excess of sodium perchlorate was added. This mixture was centrifuged and the supernatant containing the product was decanted and placed over a Spectra/Gel® Ion Exchange 1X8 column in the chloride form. The solution volume was reduced by rotary evaporation and then passed over a Whatman CM-52 cation exchange column using 0.1 M sodium hydroxide. The solution volume was again reduced, and the product was precipitated from solution by addition of a large excess of acetone. The resulting solid was collected via vacuum filtration and dried under vacuum overnight at ambient temperature.

To confirm that the desired product had been obtained (Figure 2.2C), FeTMPyP was analyzed via ^{1}H NMR spectroscopy and compared with spectra available in the literature.[4] These spectra are shown in Figure 2.4.

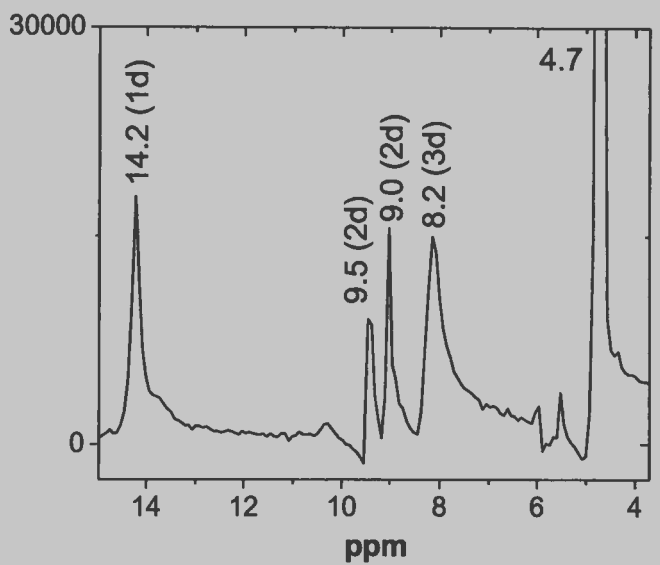

Figure 2.4. Labeled ^{1}H NMR spectra for FeTMPyP.[4] In the NMR the numbers listed above the peaks correspond to the labeled hydrogens in Figure 2.2C. The lowercase letter d denotes the μ-oxo dimeric form of the metalloporphyrin. The peak at 4.7 occurs due to HDO present from the solvent D_2O. The frequency of the spectrometer used was 400 mHz. The number of data points recorded was 8,192, with a pulse width of 6.25 μs, and an acquisition time of 34.2 ms. The recovery delay for this experiment was 20 μs, and the line broadening factor was 45 Hz.

The FeTMPyP solution contained μ-oxo dimeric FeTMPyP because its pH was 5.6. FeTMPyP has a pK_a of 5.0.[4] Above pH 5.0 the dimeric form of the metalloporphyrin will dominate, and below this the high spin monomeric form will dominate.[4] The shift at 14.2 ppm is due to the μ-oxo dimeric beta pyrrole hydrogens from the porphyrin ring. The shifts at 9.5 and 9.0 ppm are due to the ortho hydrogens of the N-methyl pyridyl ring. The shift at 8.2 ppm is caused by the meta hydrogens of the N-methyl pyridyl ring. This NMR of FeTMPyP does not exhibit a shift farther downfield as FeTPPS does because it is found

only in the μ-oxo dimeric form. The reason this shift does not occur is due to the antiferromagnetic coupling of the μ-oxo dimeric FeTMPyP.

Ni(II)PPIX

Ni(II)PPIX was purchased from Frontier Scientific Inc. and was used without further purification.

Spectrophotometric Titrations

Stability constants were determined for complexes of the three aforementioned metalloporphyrins with PhuS by spectrophotometric UV-visible absorbance titration. The titrations were carried out either by titrating an apoPhuS solution of known concentration with a titrant solution containing the respective metalloporphyrin at known concentration or by titrating a metalloporphyrin solution with a titrant solution containing apoPhuS at known concentration. PhuS and metalloporphyrin concentrations were determined spectrophotometrically based on published extinction coefficients.[5, 7] Formation of the metalloporphyrin-PhuS complexes during these titrations were tracked by the changing UV-visible absorbance spectrum between 238 and 750 nm using a commercial dual beam scanning spectrophotometer at ambient temperature.

Each titration was carried out with a solution of known PhuS concentration (which ranged from 1 to 2 μM). The concentration of the stock FeTPPS titrant solution was determined in 50 mM Tris-HCl at pH 9.0 and was based on the reported extinction coefficient of 0.93×10^{-5} $M^{-1} \cdot cm^{-1}$ at the wavelength of the Soret band maximum (Figure 2.5A).[5] The concentration of the stock solution of FeTMPyP was similarly determined in a

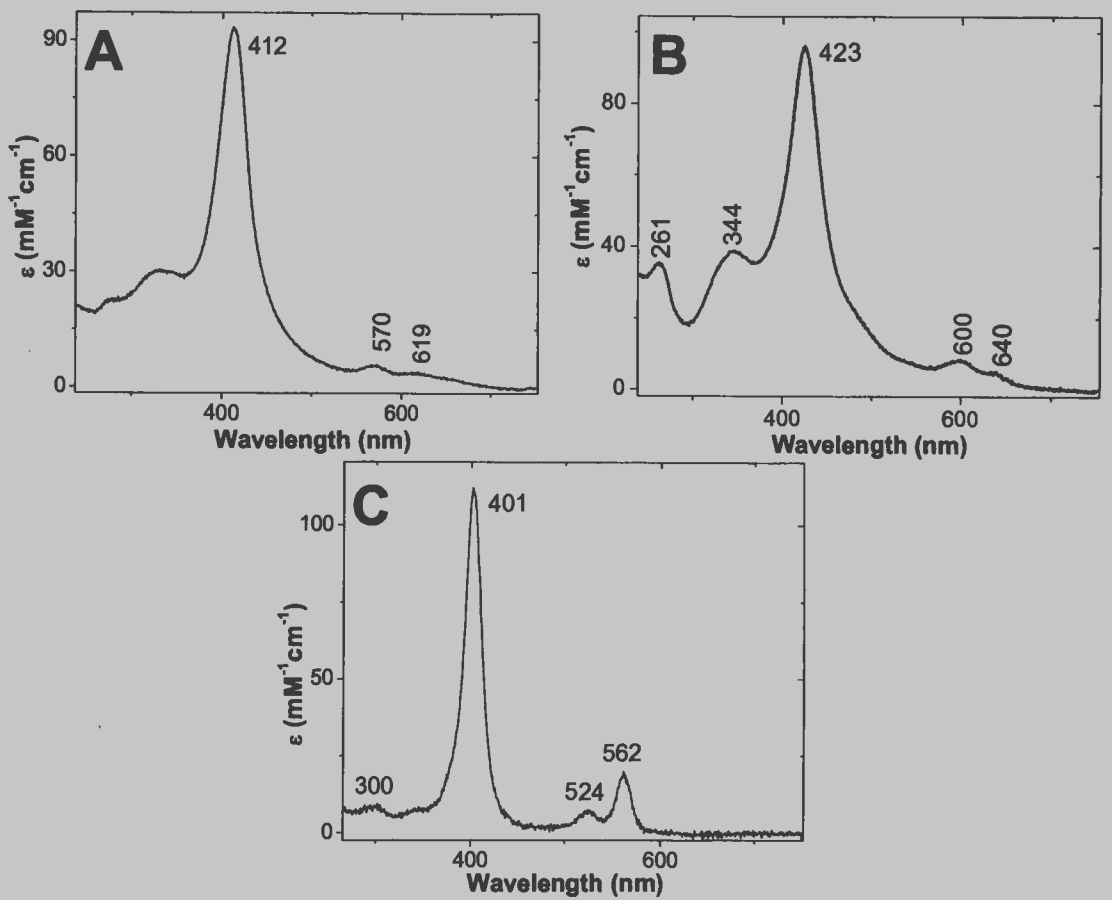

Figure 2.5. UV-visible absorbance spectra for metalloporphyrins. A) The UV-visible absorbance spectrum for FeTPPS.[4] FeTPPS exhibits a characteristic Soret absorbance band at 412 nm. Approximately 1 mg of FeTPPS was dissolved in 100 mL solution of 0.05 M Tris-HCl at a pH of 9.0. The concentration of FeTPPS was then determined by measuring the Soret absorbance and using the published extinction coefficient. [5] B) The UV-visible Absorbance spectrum for FeTMPyP.[4] FeTMPyP exhibits a characteristic Soret absorbance band at 423 nm. Approximately 1 mg of FeTMPyP was dissolved in 100 mL solution of 0.05 M Tris-HCl at a pH of 6.8. The concentration of FeTMPyP was then determined by measuring the Soret absorbance and using the published extinction coefficient.[7] C) The UV-visible absorbance spectrum for Ni(II)PPIX in DMSO. Ni(II)PPIX exhibits a characteristic Soret absorbance band at 401 nm. The concentration of Ni(II)PPIX was determined by measuring the Soret absorbance in DMSO and calculated based off of an extinction coefficient at 401 nm reported in the literature.[8]

50 mM solution of Tris-HCl at a pH of 6.8 (Figure 2.5B).[7] In preparation for titration with PhuS, Ni(II)PPIX was placed into DMSO and centrifuged for 30 minutes at 10,000 RPM to remove any particulate that was not in solution. The concentration of Ni(II)PPIX was determined spectrophotometrically in DMSO using the reported extinction coefficient of

110,700 $M^{-1} \cdot cm^{-1}$ at the Soret band maximum of 401 nm (Figure 2.5C).[8] To ensure that the reaction between the metalloporphyrins and apoPhuS had reached equilibrium, the solutions were allowed to equilibrate for 15 minutes after each addition of metalloporphyrin. The equilibrium of the reaction had been previously tested over a four hour span and the spectra remained unchanged after 10-15 minutes of the reaction had elapsed. When equilibrium had been established following each addition, the UV-visible absorbance spectrum was recorded. The titrated PhuS spectra were then subtracted from the pure iron porphyrinate spectra. The data were then analyzed by global nonlinear least squares analysis in order to determine the binding constant for the iron porphyrinate:PhuS complex.

Global Analysis Fitting Software

Global analysis software aids in the calculation of equilibrium constants through non-linear least squares analysis of the absorbance vs. titrant for each wavelength point in the spectrum using the Marquardt algorithm.[9] It yields log β values, which are the products of the stepwise equilibrium constants in the reaction. The commercial software used in this study allows the user to specify the speciation model for the titration, so that all species involved in the reaction are accounted for in the fit. It also allows known component spectra to be fixed in order to make a more constrained fit of the data. Once the desired model is input, the software will fit the data using the Marquardt algorithm in a non-linear least squares analysis. The software displays the component spectra for each species which details the molar absorptivity of each component versus wavelength. It also displays the concentration of each component versus the concentration of titrant from the fit. This gives a guided look into what occurred throughout the experiment to the concentration of each

species upon addition of the titrant solution. The software shows the titration curves at all wavelengths of the spectrum and their residuals, which show the goodness of fit. The titration curves show the fit of the actual data at every wavelength in the spectrum that was analyzed during the titration. The residual is an indicator of goodness of fit because it reveals any systematic deviations between the calculated and experimental curves, which generally suggest a less than optimum equilibrium model.

References

1. Snyder, L., *Molecular Genetics of Bacteria.* 3 ed.; ASM Press: 2007; p 735.

2. Lansky, I. B.; Lukat-Rodgers, G. S.; Block, D.; Rodgers, K. R.; Ratliff, M.; Wilks, A., The Cytoplasmic Heme-binding Protein (PhuS) from the Heme Uptake System of Pseudomonas aeruginosa Is an Intracellular Heme-trafficking Protein to the δ-Regioselective Heme Oxygenase. *Journal of Biological Chemistry* **2006,** *281* (19), 13652-13662.

3. Herrmann, O.; Mehdi, S. H.; Corsini, A., Heterogeneous metal-insertion: a novel reaction with porphyrins. *Can. J. Chem.* **1978,** *56*, 1084-7.

4. Yushmanov, V. E.; Imasato, H.; Tominaga, T. T.; Tabak, M., 1H NMR and electronic absorption spectroscopy of paramagnetic water-soluble Meso-tetraarylsubstituted cationic and anionic metalloporphyrins. *Journal of Inorganic Biochemistry* **1996,** *61* (4), 233-250.

5. Gandini, S. C. M.; Yushmanov, V. E.; Tabak, M., Interaction of Fe(III)- and Zn(II)-tetra(4-sulfonatophenyl) porphyrins with ionic and nonionic surfactants: aggregation and binding. *Journal of Inorganic Biochemistry* **2001,** *85* (4), 263-277.

6. Pasternack, R. F.; Lee, H.; Malek, P.; Spencer, C., Solution properties of tetrakis-(4-N-methyl)pyridylporphineiron(III). *Journal of Inorganic and Nuclear Chemistry* **1977,** *39* (10), 1865-1870.

7. Santiago, P. S.; Moreira, L. M.; Tabak, M., Phosphate group effects upon the equilibrium of iron(III) meso-tetrakis (4-N-methylpyridiniumyl) porphyrin in aqueous solution. *Journal of Inorganic Biochemistry* **2006,** *100* (11), 1715-1721.

8. Carr, H. S.; Tran, D.; Reynolds, M. F.; Burstyn, J. N.; Spiro, T. G., Activation of Soluble Guanylyl Cyclase by Four-Coordinate Metalloporphyrins: Evidence for a Role for Porphyrin Conformation. *Biochemistry* **2002,** *41* (31), 10149-10157.

9. Gampp, H.; Maeder, M.; Meyer, C. J.; Zuberbühler, A. D., Calculation of equilibrium constants from multiwavelength spectroscopic data--I: Mathematical considerations. *Talanta* **1985,** *32* (2), 95-101.

CHAPTER 3: RESULTS OF PHUS TITRATIONS WITH FETPPS AND FETMPYP

Introduction

Figure 2.2 in Chapter 2 shows the two synthetic metalloporphyrins, FeTPPS and FeTMPyP, whose binding to apo-PhuS was investigated by spectrophotometric titration. Both of the aforementioned iron porphyrinates were used in titrations of PhuS to investigate the feasibility of blocking the uptake of natural hemin with a competing iron complex. By virtue of their highly charged peripheral substituents, both of these iron porphyrinates are water soluble. Moreover the unmetallated porphyrins have been considered and tested as photodynamic agents for anticancer therapy.[1] Photodynamic therapy (PDT) involves the irradiation of a photosensitizer that induces production of singlet oxygen, which in turn causes cell death.[2] Thus the possibility of their use as pharmaceutical agents is reasonable to consider.

H_2TPPS has been widely tested as a PDT agent, and it was initially denied for use in therapy because of its proposed neurotoxicity in humans.[3] This was due to porphyrin impurities, because a purer sample of H_2TPPS in rats showed no neurotoxic effects.[3] It did however raise concern to nephrotoxicity, as levels of 30.8±5.5 μM/L of the porphyrin remained in the kidneys 21 days after treatment, but there appeared to be no damaging effects.[3] Levels were also relatively high in the liver (13.5±2.0 μM/L), lungs (11.7±4.6 μM/L), and spleen (9.7±1.5 μM/L), with low concentrations observed in the brain and heart.[3] The toxicity of FeTPPS and FeTMPyP was tested on hamster fibroblast cells and they were found to be largely non-toxic at concentrations ≤ 100 μM.[4]

The drug that is currently on the market for photodynamic therapy is Photofrin® which is composed of porfimer sodium, a mixture of hematoporphyrin monomers, dimers, and oligomers.[5] It has an activating wavelength of 630 nm.[5] Due to this short activating wavelength, it has only modest tissue penetrability. Therefore it is useful in the irradiation of localized tumors that are easy to access, and it has been approved by the FDA in the United States for the treatment of esophageal cancer.[5]

The metallated complexes have been shown to scavenge peroxynitrite, an oxidizing agent that is produced in inflamed tissues by reaction of ·NO with $\cdot O_2^-$.[6] The iron in FeTPPS forms an oxo-iron (IV) complex upon binding to the distal oxygen in peroxynitrite.[7] This binding catalyzes the isomerization of peroxynitrite to nitrate by causing a nitrogen dioxide to exit.[7] Quinolinic acid, a neurotoxin that has been found in increased concentration in the brains of patients with Alzheimers, Huntington's, and Parkinson's disease has been shown to cause an increase in peroxynitrite within the brain.[6] FeTPPS has been shown to decrease cytoxicity in the brain of rats, through the scavenging of peroxynitrite.[7] So it could therefore be used as a potential treatment for these diseases through scavenging peroxynitrite produced by quinolinic acid.[7]

FeTPPS and FeTMPyP exhibit rich acid-base speciation in aqueous solution, which is depicted in a cartoon representation in Figure 3.1. Figure 3.1A shows a cartoon representation of the speciation of FeTPPS, which exhibits three main species in aqueous solution whose fractional populations vary as a function of pH depicted in Figure 1B.[8] At $pH \leq 4.7$, FeTPPS is monomeric and pentacoordinate with an axial water ligand (Component I).[8] At pHs between 4.7 and 10.4, FeTPPS is predominantly μ-oxo dimeric (Component II) in solution, and at $pH > 10.4$, FeTPPS is monomeric and pentacoordinate

with an axial hydroxide ligand (Component III).[8] At a pH of 8.0 where the PhuS titrations with FeTPPS were performed, the concentration of μ-oxo dimer is approximately 90%, while the remaining speciation is accounted for by the hydroxyl monomer at 10% in solution.

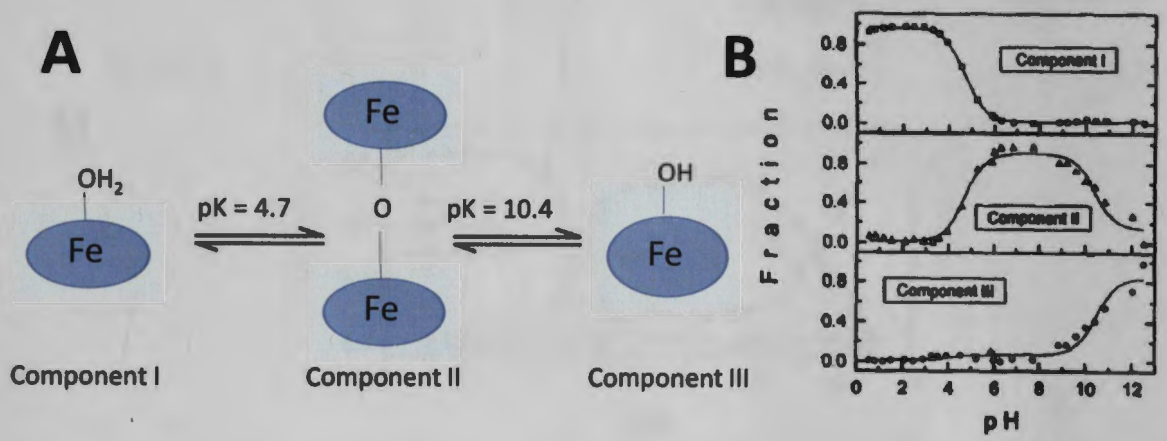

Figure 3.1. Acid base speciation of FeTPPS. (A) Cartoon representation of the acid-base speciation of FeTPPS. (B) Fraction of each component in solution versus pH.[8]

Figure 3.2A shows the acid-base speciation of FeTMPyP and Figure 3.2B shows a fractionation plot of each species of FeTMPyP present in solution versus pH. FeTMPyP is monomeric with a single water ligand at pH ≤ 4 (Species 1).[9] It is predominantly μ-oxo dimer (Species 2) between pH of 5 and 10, and above pH 11 it is monomeric and hexacoordinate with a bis-hydroxo axial ligand set (Species 3).[9] At a pH of 8.0 where the titrations with PhuS were being performed, the μ-oxo dimeric compound is present at approximately 83%, with the bis-hydroxyl monomer encompassing the other 17% in solution. Interestingly by virtue of its large positive charge, the first example of a bis-hydroxo iron porphyrinate was identified and characterized in the 2-N-methylpyridyl analogue of FeTMPyP.[10]

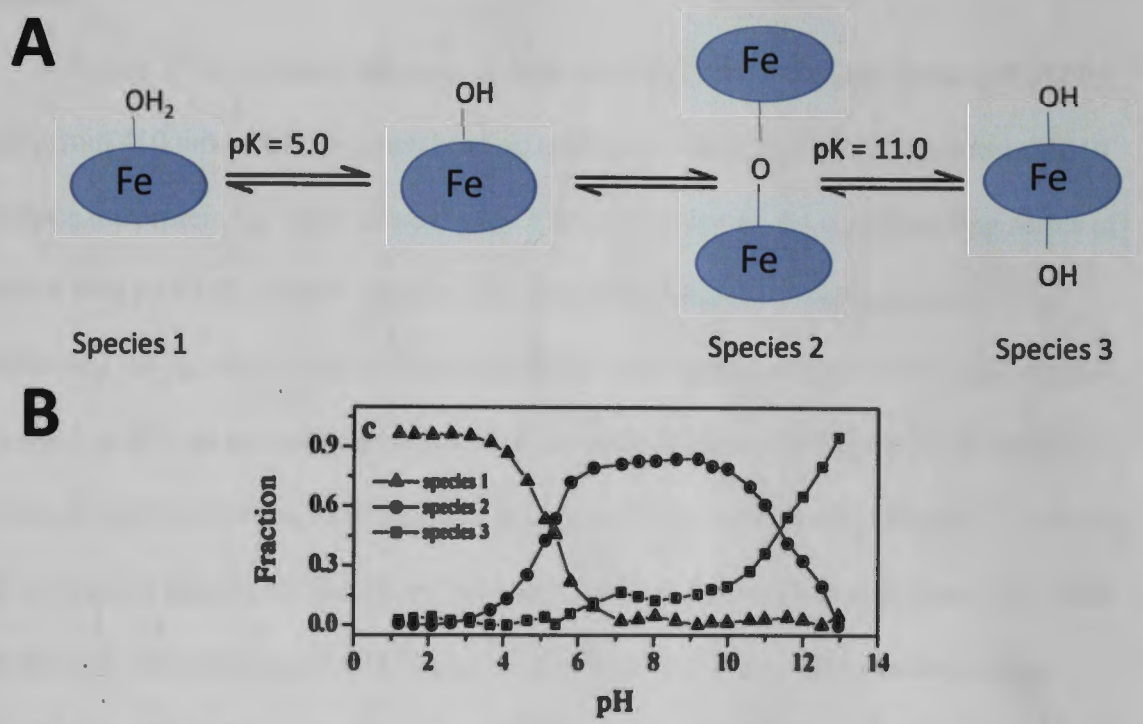

Figure 3.2. Acid base speciation of FeTMPyP. (A) Cartoon representation of the acid-base speciation of FeTMPyP. (B) Fraction of each species in solution versus pH.[11]

The binding of these compounds with bacterial heme trafficking proteins are of general interest because of their potential to block or inhibit heme internalization and/or intracellular transport. As prospective pharmaceutical agents, they are attractive because of their ease of preparation. In order to explore the influence of peripheral charge on nonbonded interactions between the porphyrin and protein, iron porphyrinates having positively and negatively charged peripheries have been investigated. FeTPPS carries a negative charge on each sulfonato group at a physiological pH, while FeTMPyP carries a positive charge on each N-methyl-4'-pyridyl group. These two metalloporphyrins contain bulkier side chains than does FePPIX. Nevertheless as shown in this chapter, both appear to form stable complexes with PhuS at near physiological pH.

Results

Figure 3.3A shows the titration of PhuS with FeTPPS. The Soret band of FeTPPS shifts from 410 nm to 426 nm upon binding to PhuS and then shifts back out towards 410 nm once the protein has become saturated. Figure 3.3B shows the corresponding series of spectra with no PhuS present. Figure 3.3C shows the difference spectra calculated by subtracting the spectra in Figure 3.3B from their counterparts in Figure 3.3A. The negative ΔA band at 405 nm corresponds to the disappearance of free FeTPPS, while the positive ΔA band at 438 nm arises from its appearance in the PhuS binding site. Figure 3.3D shows the component spectra for the global nonlinear least squares analysis of Figure 3.3A. The spectrum for the monomeric FeTPPS exhibits a Soret at 395 nm. This spectrum was recorded at pH 4 and fixed to help constrain the fit. The spectrum for the μ-oxo dimer exhibits a Soret maximum at 412 nm. At pH 8.0, FeTPPS is approximately 90% μ-oxo dimer and 10% monomer with a single axial hydroxide ligand. The spectrum of μ-oxo dimer that was used to constrain the fit was obtained by subtracting the contribution of the high-pH monomeric species from the spectrum of FeTPPS recorded at pH 8.0. The log β for formation of the μ-oxo dimer was then fixed at 8.1 in accord with its reported value at pH 8.0.[8, 12] The spectrum of the monomeric hydroxide complex exhibits a Soret maxiumum at 424 nm. This spectrum was recorded at pH 13 and used to constrain the fit at a log β value of 7.0.[13] FeTPPS binds to PhuS in a 1:1 mole ratio ([FeTPPS]:[PhuS]). The global analysis software yielded the component spectrum for the [FeTPPS]:[PhuS] which exhibits a Soret maximum at 424 nm, consistent with the Soret position in the spectrum after the first titrant addition to PhuS.

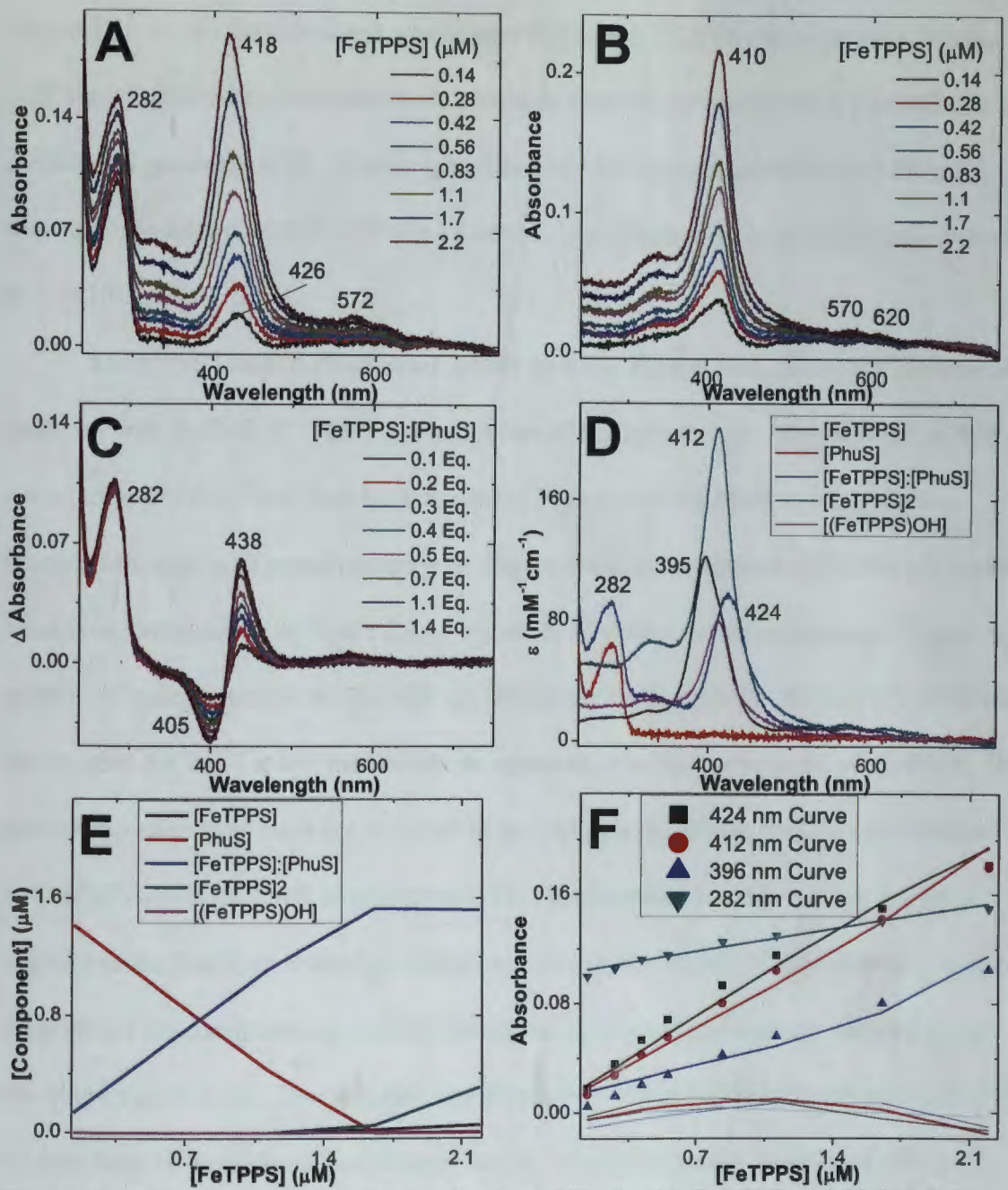

Figure 3.3. UV-visible spectra for the titration of PhuS with FeTPPS and Global fitting analysis. (A) UV-Visible titration data for [FeTPPS]:[PhuS]. (B) UV-Visible spectra of pure FeTPPS measured in additions equal to data collected in A. (C) Typical titration subtraction data for FeTPPS and PhuS. The peak at 282 nm is PhuS, the peak at 405 nm is the unbound FeTPPS, and the peak at 438 nm is PhuS bound to FeTPPS. FeTPPS began to precipitate out of solution after 3 equivalent amounts had been added, so data collected after this point was not included in further analysis. (D) Global analysis calculated component spectra. (E) Global analysis calculated concentration spectra. The component spectra show each species present in the titration. (F) The titration curves, fit to the data, and calculated residuals show the goodness of fit at the indicated wavelengths.

Figure 3.3E shows the calculated speciation versus total FeTPPS concentration. Figure 3.3F shows selected experimental and calculated titration curves and their residuals, as an indicator of goodness of fit. The weighted average of the log β values for the three titrations of apoPhuS with FeTPPS is 11.66 ± 1.7, corresponding to a dissociation constant of $2.2 \times 10^{-12} \pm 0.02$ M.

FeTMPyP binds to PhuS in a 1:1 ratio as well. Figure 3.4A shows the titration of apoPhuS with FeTMPyP. The Soret maximum of FeTMPyP shifts from 424 nm to 446 nm upon binding to PhuS and then back towards 424 nm once the PhuS binding site has become saturated with metalloporphyrin. Figure 3.4B shows spectra of FeTMPyP at the same concentrations as in Figure 3.4A. Figure 3.4C shows the corresponding difference spectra. The negative ΔA band at 420 nm shows the disappearance of free FeTMPyP while the positive ΔA band at 453 nm reveals its appearance in the binding site of apoPhuS. The spectra shown in gray were not included in the analysis because at these concentrations FeTMPyP caused the PhuS to precipitate. This precipitation is evidenced by the large increase in the Rayleigh scattering background in the blue region of the spectrum. Figure 3.4D shows the component spectra for the global nonlinear least squares analysis of the spectra in Figure 3.4A. The spectrum for the acidic form of FeTMPyP was recorded at pH 1.0 and fixed in the analysis to constrain the fit. It exhibits a split Soret band with a maximum absorbance at 405 nm and a shoulder at 420 nm. The spectrum of the μ-oxo dimer exhibits a Soret maximum at 423 nm. At a pH of 8.0, FeTMPyP is about 83% μ-oxo dimer and 17% bishydroxo-monomer. The spectrum of the μ-oxo dimer that was fixed in order to constrain the fit was generated by subtracting the contribution of the bishydroxyl-monomer spectrum from the pH 8.0 spectrum of the FeTMPyP.

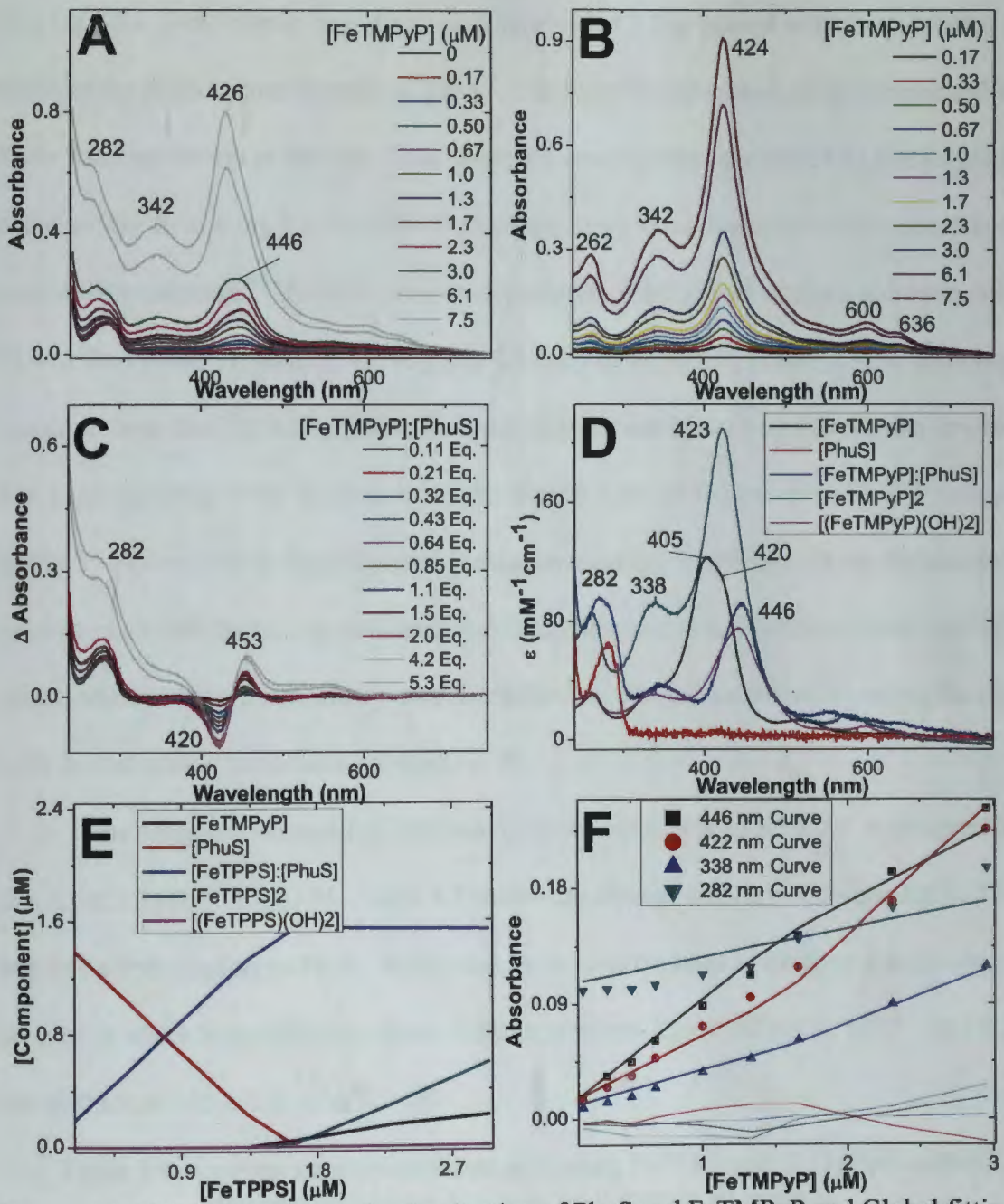

Figure 3.4. UV-visible spectra for the titration of PhuS and FeTMPyP and Global fitting analysis. (A) UV-Visible titration data for [FeTMPyP]:[PhuS]. (B) UV-Visible spectrum of pure FeTMPyP measured in equal additions to data collected in A. (C) Typical titration subtraction data for FeTMPyP and PhuS. The peak at 282 nm is PhuS, the peak at 420 nm represents the free FeTMPyP, and the peak at 453 is PhuS bound to FeTMPyP. FeTMPyP began to precipitate out of solution after 1 equivalent had been added, so spectra after this point were not included in further analysis. (D) Global analysis calculated component spectra. (E) Global analysis calculated concentration spectra. (F) The titration curves, fit to the data, and calculated residuals show the goodness of fit at the indicated wavelengths. The data shown in gray was not included in the global analysis.

The log β for μ-oxo dimer formation was then fixed at 7.1 in accord with the published value of the dimerization constant at pH 8.[9] The bishydroxyl-monomer spectrumexhibits a Soret band maximum at 446 nm. This spectrum was recorded at a pH of 13 and used to constrain the fit at a log β value of 11.9, corresponding to the formation of the bishydroxyl-monomer in solution.[9] The sole calculated spectrum of the global analysis software in this fit was the FeTMPyP binding to PhuS in a 1:1 ratio ([FeTMPyP]:[PhuS]). The component spectrum from the [FeTMPyP]:[PhuS] fitting analysis exhibits a Soret maximum at 446 nm, corresponding to the Soret maximum in Figure 3.4A of 446 nm of FeTMPyP binding to PhuS. Figure 3.4E is the calculated speciation diagram, which reveals the fractional populations of all the species occurring during the titration as a function of total FeTMPyP concentration. Figure 3.4F shows calculated titration curves at selected wavelengths along with their residuals to indicate goodness of fit.

The weighted average log β values for four titrations is 11.65 ± 2.3, corresponding to a K_d of $2.2 \times 10^{-12} \pm 0.01$ M. Table 3.1 shows the average stability constants for FeTPPS and FeTMPyP binding to PhuS. Hemin has been found to bind to PhuS by a stepwise process in which heme:$(PhuS)_2$, forms with an apparent $K_d = 0.10 \pm 0.01$ μM.[14] The K_d for heme:PhuS is 0.40 ± 0.02 μM.[14]

Table 3.1. Average stability constants of binding FeTPPS and FeTMPyP to PhuS determined through nonlinear least squares fit analysis.

Type of Titration	Titrant Solution	Fitting Model	Average Stability Constant (M)
PhuS with FeTPPS	FeTPPS	FeTPPS:PhuS	$2.2(\pm 0.02)\times10^{-12}$
PhuS with FeTMPyP	FeTMPyP	FeTMPyP:PhuS	$2.2(\pm 0.01)\times10^{-12}$

As evidenced by Figure 3.4C, a stoichiometric excess of FeTMPyP causes PhuS to precipitate out of solution. The isoelectric point of PhuS is 5.4, so it is at this pH that the

protein carries no net charge.[15] So at pH of 8.0, as in this experiment, PhuS carries an overall negative charge. Thus it is likely that the negatively charged protein is precipitated from solution by excess FeTMPyP, which carries a 4+ charge at pH 8.0.

Discussion

The results of this experiment reveal that synthetic metalloporphyrins are able to bind to PhuS. These data analyses of metalloporphyrin binding to PhuS were novel because they incorporated all porphyrin species that existed in solution with the protein into the fit of the data. It is not clear if these porphyrins have a higher binding affinity for PhuS than heme, because its apparent binding constant does not currently account for the π-π dimerization of free hemin in aqueous solution.[16] At a pH of 8.0, the dissociation constant for the π-π dimerization of free hemin is 2.6×10^{-7}.[17] An accounting for the energetic cost of dissociating the hemin dimer reveals a similarly large stability of native holoPhuS of approximately 1×10^{-13} M.

FeTPPS and FeTMPyP both contain iron so they are able to form proximal histidine bonds with PhuS. At neutral pH PhuS has an overall negative charge, so it is interesting that it has the same binding affinity for the negatively charged FeTPPS and the positively charged FeTMPyP. It would seem that PhuS should have a lower affinity for FeTPPS, but PhuS does contain positively charged lysine and arginine amino acid side chains that normally interact with heme propionate groups, so it could be interacting with these residues.

The stoichiometric association of both iron porphyrinates with PhuS argues for specific binding, possibly in the native heme binding site. However these results do not provide any direct evidence that the native site is populated. In order to see if FeTPPS and

FeTMPyP are binding in the same site as hemin, the protein's passage of metalloporphyrin to heme oxygenase could be analyzed. If the metalloporphyrin was passed from PhuS to heme oxygenase this would be consistent with the iron porphyrinate occupying the native PhuS binding site. If the metalloporphyrin was not being transferred to heme oxygenase this could indicate potential as a pharmaceutical agent in order to inhibit bacterial heme uptake.

Future work will also include determining the affinity of PhuS(H109A) for the iron porphyrinates to see whether lack of the native distal heme ligand diminishes the stability of the heme-protein complex, as would be expected if the Fe-His bond could not form. Additionally, NMR and CD spectroscopic studies of the metalloporphyrins bound to PhuS. NMR spectroscopy could give some insight insofar as seeing which residues are most affected by contact with the protein and their dipolar shifts to see if they are similar to hemin or other metalloporphyrins. Circular dichroism (CD) spectroscopy analyses would show how the secondary structure of the protein changes upon binding to FeTPPS and FeTMPyP. It would also be of further interest to obtain a crystallographic structure for this metalloporphyrin:protein complex to see how the metal in the ring was coordinated to the protein as well as how the bulky ring constituents were oriented upon binding to PhuS.

References

1. Dedic, R.; Vyklický, V.; Svoboda, A.; Hála, J., Phosphorescence of singlet oxygen and 5,10,15,20-tetrakis(1-methyl-4-pyridinio)porphine: Time and spectral-resolved study. *Journal of Molecular Structure* **2009,** *924-926*, 153-156.

2. Ion, R.-M., Photodynamic therapy (PDT): a photochemical concept with medical applications. *Rev. Roum. Chim.* **2008,** *52*, 1093-1102.

3. Zima, T.; Jirsa, M.; Jirsa, M., Jr.; Bradova, V.; Stejskal, J.; Zabka, J.; Povysil, C.; Janebova, M., The localization of TPPS4 in some organs and its possible nephrotoxicity in rats. *Physiol. Res. (Prague)* **1997,** *46*, 351-355.

4. O'Hara, J. A.; Douple, E. B.; Abrams, M. J.; Picker, D. J.; Giandomenico, C. M.; Vollano, J. F., Potentiation of radiation-induced cell kill by synthetic metalloporphyrins. *International Journal of Radiation Oncology, Biology, Physics* **1989,** *16* (4), 1049-1052.

5. Moreira, L. M.; dos, S. F. V.; Lyon, J. P.; Maftoum-Costa, M.; Pacheco-Soares, C.; da, S. N. S., Photodynamic Therapy: Porphyrins and Phthalocyanines as Photosensitizers. *Aust. J. Chem.* **2008,** *61*, 741-754.

6. Lee, J.; Hunt, J. A.; Groves, J. T., Mechanisms of Iron Porphyrin Reactions with Peroxynitrite. *Journal of the American Chemical Society* **1998,** *120* (30), 7493-7501.

7. Klassen, S. S.; Rabkin, S. W., The metalloporphyrin FeTPPS but not by cyclosporin A antagonizes the interaction of peroxynitrate and hydrogen peroxide on cardiomyocyte cell death. *Naunyn-Schmiedeberg's Arch. Pharmacol.* **2009,** *379*, 149-161.

8. Yushmanov, V. E.; Imasato, H.; Tominaga, T. T.; Tabak, M., 1H NMR and electronic absorption spectroscopy of paramagnetic water-soluble Meso-tetraarylsubstituted cationic and anionic metalloporphyrins. *Journal of Inorganic Biochemistry* **1996,** *61* (4), 233-250.

9. Santiago, P. S.; Gandini, S. C. M.; Tabak, M., Spectroscopic studies of the interaction of cationic water-soluble iron(III) meso-tetrakis(4-N-methylpyridiniumyl)porphyrin (FeTMPyP) with ionic and nonionic micelles. *J. Porphyrins Phthalocyanines* **2005,** *9*, 94-108.

10. Rodgers, K. R.; Reed, R. A.; Su, Y. O.; Spiro, T. G., Resonance Raman and magnetic resonance spectroscopic characterization of the Fe(I), Fe(II), Fe(III), and Fe(IV) oxidation states of Fe(2-TMPyP)n+(aq). *Inorganic Chemistry* **1992,** *31* (13), 2688-2700.

11. Santiago, P. S.; Gandini, S. C. M.; Tabak, M., Spectroscopic studies of the interaction of cationic water-soluble iron(III) meso-tetrakis(4-N-methylpyridiniumyl)porphyrin (FeTMPyP) with ionic and nonionic micelles. *J. Porphyrins Phthalocyanines* **2005,** *9* (Copyright (C) 2010 American Chemical Society (ACS). All Rights Reserved.), 94-108.

12. Fleischer, E. B.; Palmer, J. M.; Srivastava, T. S.; Chatterjee, A., Thermodynamic and kinetic properties of an iron-porphyrin system. *J Am Chem Soc* **1971,** *93*, 3162-7.

13. El-Awady, A. A.; Wilkins, P. C.; Wilkins, R. G., Kinetic aspects of the iron(III)-tetrakis(p-sulfonatophenyl)porphine system. *Inorganic Chemistry* **1985,** *24* (13), 2053-2057.

14. Block, D. R.; Lukat-Rodgers, G. S.; Rodgers, K. R.; Wilks, A.; Bhakta, M. N.; Lansky, I. B., Identification of Two Heme-Binding Sites in the Cytoplasmic Heme-Trafficking Protein PhuS from Pseudomonas aeruginosa and Their Relevance to Function. *Biochemistry* **2007,** *46* (50), 14391-14402.

15. Ochsner, U. A.; Johnson, Z.; Vasil, M. L., Genetics and regulation of two distinct haem-uptake systems, phu and has, in Pseudomonas aeruginosa. *Microbiology* **2000,** *146* (1), 185-198.

16. Block, D. R. Biophysical Studies of Heme Assimilation Proteins from Pathogenic Bacteria. NDSU, Fargo, ND, 2009.

17. de Villiers, K.; Kaschula, C.; Egan, T.; Marques, H., Speciation and structure of ferriprotoporphyrin IX in aqueous solution: spectroscopic and diffusion measurements demonstrate dimerization, but not μ-oxo dimer formation. *Journal of Biological Inorganic Chemistry* **2007,** *12* (1), 101-117.

CHAPTER 4: RESULTS OF NI(II)PPIX TITRATIONS WITH PHUS

Introduction

Nickel(II) Protoporphyrin IX (Ni(II)PPIX) was used in spectrophotometric titrations with PhuS, a cytoplasmic heme trafficking protein from *P. aeruginosa*. Ni(II)PPIX was chosen for this study because the Ni(II) center is square planar and will interact only weakly with the proximal His residue within the heme-binding pocket of PhuS. Through analyzing the binding of Ni(II)PPIX to the pocket of PhuS, the properties of the non-iron peripheral binding of the PPIX ring to PhuS can be assessed. Therefore the results of these titrations can give an idea of the importance of non-iron bonds that are forming between the protoporphyrin IX ring of heme and PhuS.

The structure of Ni(II)PPIX is depicted in Figure 4.1. Its formula weight is 621.35 g/mol, and it is not an oxygen reactive complex.[1] Nickel(II) has a smaller ionic radius than iron(II). Thus the Ni-N bonds in the center of the porphyrin macrocycle are shorter than the analogous Fe-N bonds of heme.[2] This contraction of the porphine core results in an equilibrium out of plane distortion known as ruffling, in which opposing pyrrole rings are counter rotated about their Ni-N bond axes.[3]

Nickel(II) has a strong tendency to form square planar coordination complexes with strong field ligands. The square planar geometry is electronically stabilized by the low spin d^8 configuration illustrated in Figure 4.2. The filled d_z^2 based molecular orbital is σ antibonding with respect to axial ligands. Thus low-spin axial Ni-L σ bonds are generally quite weak and axial ligands tend not to bind.[2] As depicted in Figure 4.2 the energy gap between the filled d_{xy} and the empty $d_{x^2-y^2}$ orbital is large. Among the consequences of

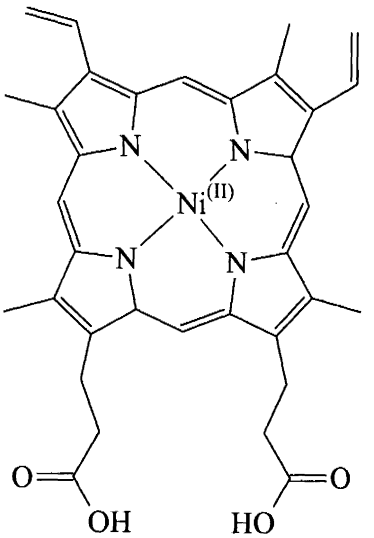

Figure 4.1. Stick structure of Ni(II)PPIX. The $PPIX^{2-}$ ligand is a tetrapyrrolic macrocycle. It comprises a 22 π electron aromatic ring and eight functional groups of three types: two vinyl, two propionyl (pKa 4.87)[4], and four methyl. The four pyrrole nitrogen atoms in the porphyrinate core provide the square planar coordination environment for Ni(II).

these electronic properties are that, in contrast to heme, the Ni(II) center resists oxidation and reduction and it does not readily bind axial ligands.

Therefore Ni(II)PPIX was chosen for this PhuS binding study to gain insight into the contributions of non-bonding interactions between the protoporphyrin IX ring and PhuS to the driving force for association.

It has been demonstrated that proteins can perturb the Ni(II)PPIX conformation. For example in hemoglobin and myoglobin that have been reconstituted with Ni(II)PPIX, the Ni(II)PPIX complex exhibits a doming distortion.[5] This distortion from the square planar geometry can impart modest stability to axial Ni-ligand bonds.[5] If there is a large excess of certain ligands in a solution of Ni(II)PPIX, this can result in axial ligation of the nickel center as well.[6] This behavior has been shown in solutions of synthetic Ni(II) octaethyl porphyrins containing pyridine.[6]

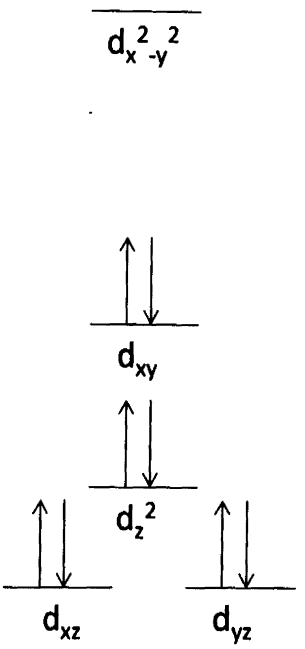

Figure 4.2. Ligand field splitting diagram for square planar d^8 complexes.[7]

The speciation of Ni(II)PPIX in aqueous solution remains unreported, unlike the speciation in aqueous solution of FeTPPS and FeTMPyP from the previous chapter. However it has long been known that porphyrins and metalloporphyrins aggregate in aqueous solution.[8] It was determined that protoporphyrin forms face-to-face aggregates with itself in solutions with polar solvents.[9] In these aggregates the porphyrin arrangement is such that the vinyl groups are oriented toward the inside of the porphyrin aggregate due to their hydrophobicity. In contrast the propionate substituents are more solvent exposed due to their hydrophilicity.[9] Alcohol commonly causes the disruption of aqueous organic dye aggregates, including the porphyrins.[8, 10] This is attributed to the reduced dielectric constant of the water-alcohol mixture.[11] Due to its behavior in a Beer's law plot of absorbance vs. concentration, Ni(II)PPIX dimethyl ester (DME) in twenty percent aqueous ethanol was thought to be an aggregate, because at concentrations > $1x10^{-5}$ M, the metalloporphyrin deviated from Beer's Law.[12] Another sign that aggregation was

occurring in the sample was the fact that when the ethanol concentration in the sample was changed from twenty to fifty percent, the absorbance of the porphyrin doubled.[12] The dimerization constant for Ni(II)PPIX-DME in twenty percent ethanol is $1x10^6$ M^{-1}.[12]

The extent of porphyrin and metalloporphyrin dimerization or higher aggregation depends upon the solvent, pH, ionic strength, temperature, and concentration. Porphyrins in neutral solutions tend to aggregate more than those in acidic solutions.[8] As the temperature increases, porphyrins tend to become less aggregated, consistent with a negative entropy of self association.[13] The extent of aggregation generally tracks the ionic strength of a solution.[8] Also it has been shown that porphyrins containing sterically bulky substituents are less driven to aggregate.[8]

Hemin or Fe(III)PPIX has been found to exist as a monomer, μ-oxo-dimer, π-π dimer, and π-stacked aggregates of μ-oxo-dimers depending on the solvent, pH, ionic strength, and temperature of the solution.[14] In contrast there is not evidence for μ-oxo dimerization of Ni(II)PPIX. Ni(II)PPIX forms π-π dimers and probably higher π-stacked aggregates.[12]

Results

Ni(II)PPIX is soluble and monomeric in DMSO with a sharp Soret maximum at 401 nm. Because Ni(II)PPIX is only sparingly soluble in water, it needs to be solvated in DMSO before it can be diluted into an aqueous solution. Upon addition to aqueous solution Ni(II)PPIX self associates. The Soret band for these solutions is broad with its maximum occurring at 380 nm. In contrast the UV-visible spectrum of Ni(II)PPIX in DMSO remained unchanged over the course of at least one week at ambient temperature. However once Ni(II)PPIX in DMSO was diluted into an aqueous solution it slowly

precipitated with loss of extinction at the Soret band maximum that was logarithmic in time (Figure 4.3).

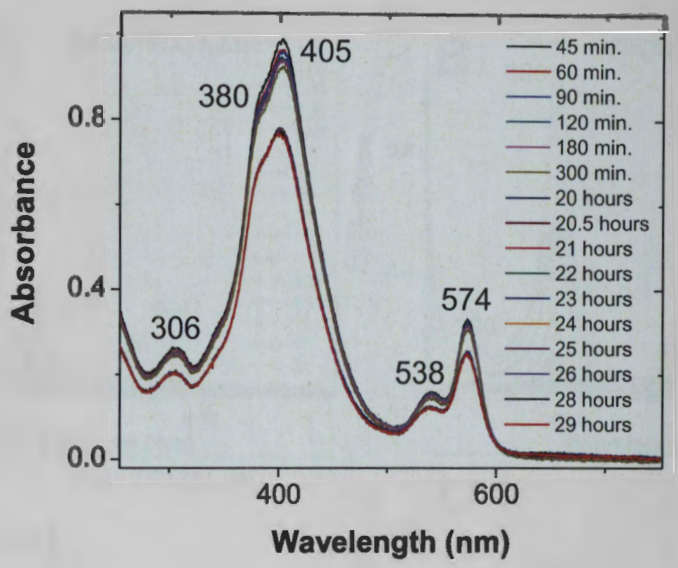

Figure 4.3. UV-visible absorbance spectra of Ni(II)PPIX in aqueous solution over time. Ni(II)PPIX was at a concentration of 33 μM in an aqueous solution of 25 mM triethanolamine. The solution was centrifuged at 10,000 RPM for 30 minutes immediately before being analyzed via UV/Vis spectroscopy at 45 minutes. The solution was then centrifuged again at 10,000 RPM for 30 minutes at about 19.5 hours and the absorbance of the Ni(II)PPIX dropped significantly.

The solution was then centrifuged and analyzed again over time to reveal a slower precipitation. It is evident from the spectral changes upon addition of Ni(II)PPIX to PhuS that binding is occurring (vide infra). However due to the complexity of Ni(II)PPIX speciation in aqueous solution, neither the extent of aggregation nor the distribution of aggregates is clear. Thus under physiologically relevant conditions, it does not appear possible to accurately determine the intrinsic stability of Ni(II)PPIX:PhuS. Therefore as will be further explained below, the stability constants reported here must be considered approximate.

Two variations of the spectrophotometric titration were performed with the goal of determining the thermodynamic stability of PhuS loaded with Ni(II)PPIX. Figure 4.4 shows a typical set of UV-visible spectra that track the spectrophotometric titration of PhuS

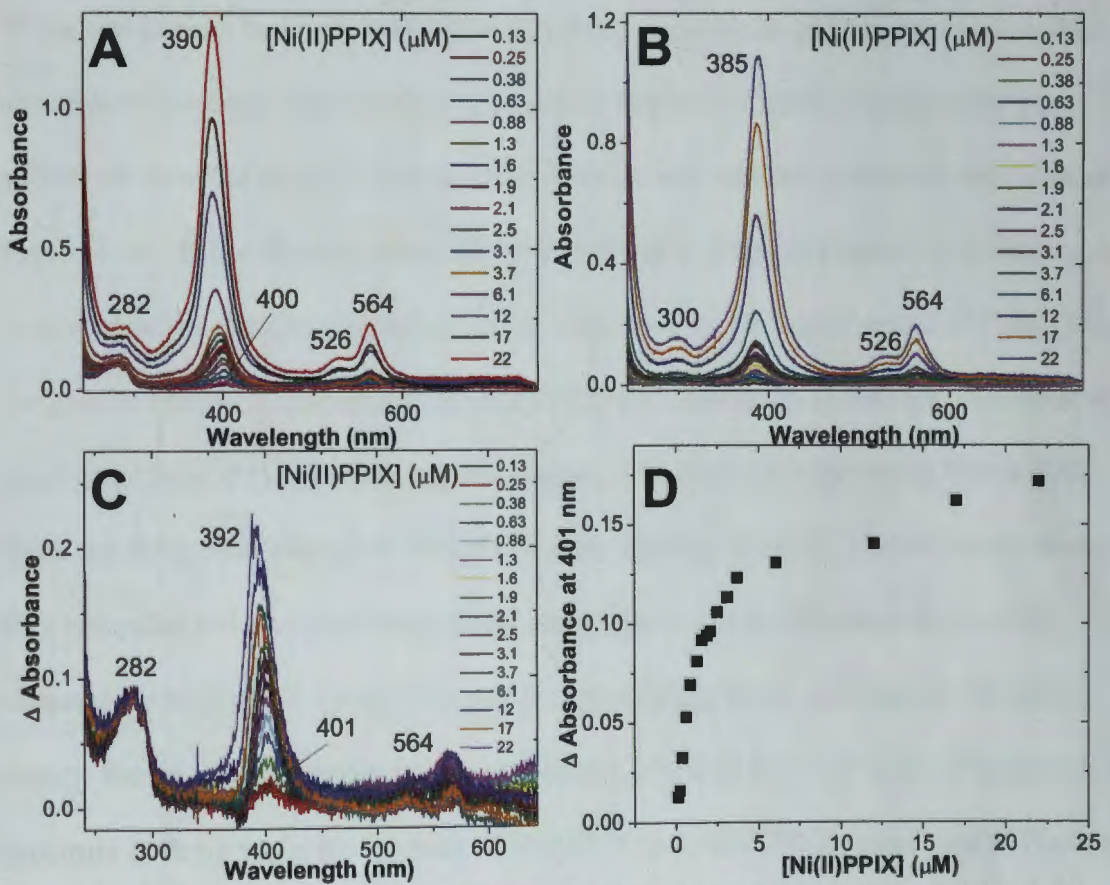

Figure 4.4. UV-visible spectra for the titration of PhuS and Ni(II)PPIX. A) UV-visible spectra of aqueous Ni(II)PPIX from 0.13 to 22 μM. B) A typical titration of Ni(II)PPIX and PhuS from 0.1 to 20 Eq. of Ni(II)PPIX to PhuS into 50 mM Tris-HCl pH = 8.0. The concentration of PhuS in this solution was 1.3 μM. C) The difference spectrum of Figure 4 subtracted from Figure 3 for the Ni(II)PPIX and PhuS titration. D) Plot of ΔA at 401 nm from Figure 4C versus concentration of Ni(II)PPIX titrated into solution.

with Ni(II)PPIX. The Ni(II)PPIX titrated into aqueous solution was predominantly aggregated as evidenced by the maximum Soret band at 385 nm. Each titration of this type involved adding aliquots of a standard Ni(II)PPIX solution to an apo-PhuS solution of known concentration (typically between 1 and 2 μM). It was important to allow sufficient

time for the system to reach equilibrium following each addition of titrant. The equilibration time was ten minutes, which was determined empirically by monitoring the absorbance spectrum after addition of Ni(II)PPIX until change could no longer be detected. When equilibrium had been established following each titrant addition, the UV-visible absorbance spectrum was recorded. The pure Ni(II)PPIX spectra (Figure 4.4B) were subtracted from the titrated PhuS spectra (Figure 4.4A), and this difference data is shown in Figure 4.4C. In the first few additions of Ni(II)PPIX to PhuS in Figure 4.4A, binding can be evidenced by the metalloporphyrin due to the monomeric Soret band at 401 nm. Once the protein sample is saturated with Ni(II)PPIX, the Soret shifts to 390 nm, consistent with aggregated Ni(II)PPIX dominating the mixture. The difference spectra in Figure 4.4C show the Soret band change of Ni(II)PPIX upon binding to PhuS. The difference data were then compiled and analyzed using global analysis in order to determine the stability constant for Ni(II)PPIX:PhuS. The results of this fit are shown in Figure 4.5A, which depicts the $\Delta\varepsilon$ versus wavelength of each species involved in the titration. The protein spectrum is fixed, while the monomer Ni(II)PPIX and Ni(II)PPIX complexed to PhuS are calculated by the analysis algorithm. Figure 4.5B is the speciation plot which shows the calculated concentration of each component versus the total Ni(II)PPIX concentration. The experimental and calculated titration curves at a few selected wavelengths are shown in Figure 4.5C, along with their corresponding residuals. The average apparent stability constant for Ni(II)PPIX:PhuS is $3.2(\pm 0.6)\text{x}10^{-7}$ M. However it is evident from Figure 4.4D, in the plot of the ΔA at 401 nm of Figure 4.4C versus the concentration of Ni(II)PPIX titrated into solution, that the speciation of Ni(II)PPIX is more complex than a

simple 1:1 binding ratio of Ni(II)PPIX:PhuS in solution. Figure 4.4D suggests that spectral change continues with increasing Ni(II)PPIX concentration. Given the aforementioned

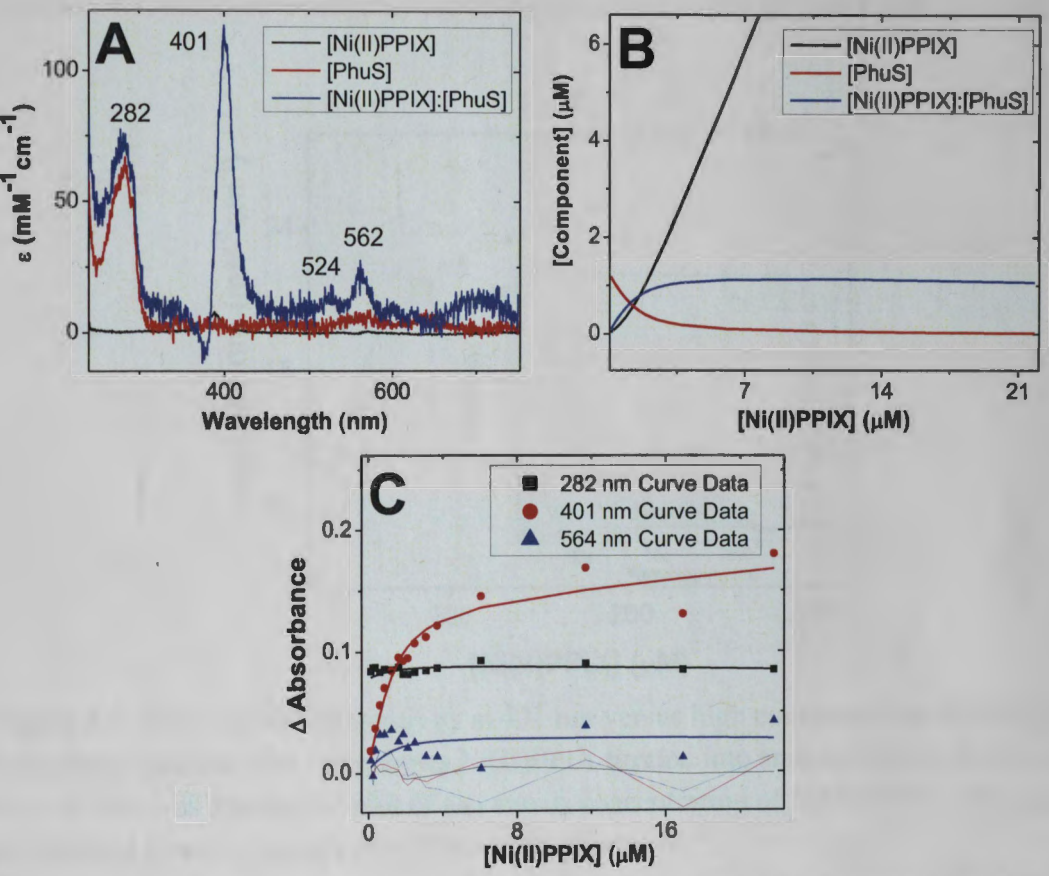

Figure 4.5. Global fitting analysis of the titration of PhuS with Ni(II)PPIX. Depicted are the results for the fit of the data in Figure 4C. (A) Calculated component spectra. (B) Calculated concentration spectra. (C) The titration curves, fit to the data, and calculated residuals show the goodness of fit at the indicated wavelengths. The data were fit to a 1:1 model of [Ni(II)PPIX]:[PhuS].

propensity for metalloporphyrin aggregation in aqueous solution, it was hypothesized that a $(Ni(II)PPIX)_2$ dimer was being formed at higher titrant concentrations.

To test this hypothesis absorbance spectra of Ni(II)PPIX were recorded over a concentration range from ~10^{-9} to ~10^{-4} M. The concentration dependence of the Ni(II)PPIX speciation was assessed by analyzing a plot of ε_{401} vs. $[NiPPIX]_{total}$. Because the exact speciation is not clear, the assumption was made that only monomeric and

dimeric Ni(II)PPIX species of were present in solution. That plot, which is shown in Figure 4.6, was analyzed by nonlinear least squares fitting. The fitting function is shown in Equation 4.1, and it accounts only for an equilibrium mixture of dimer and monomer.[15]

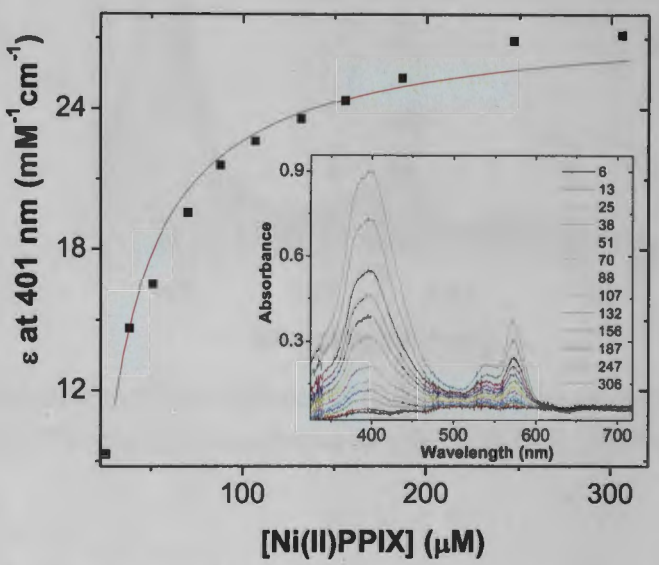

Figure 4.6. Plot of molar absorptivity at 401 nm versus high concentration of Ni(II)PPIX in aqueous solution. The inset shows Ni(II)PPIX titrated into aqueous solution from 6 to 306 μM that was used in the plot of ε_{401} versus concentration of Ni(II)PPIX. The data is fit to a derived function using a non-linear least squares fit.[15]

$$y = A_1 + A_2\left(\frac{(4A_3x - 1) + ((4A_3x - 1)^2 - 16A_3^2x^2)^{\frac{1}{2}}}{8A_3x}\right)$$

Equation 4.1. Fitting function for dimeric constant calculation of Ni(II)PPIX. In this equation, x is the total concentration of Ni(II)PPIX, y is the total molar absorptivity constant, A_1 is the extinction coefficient for the monomeric species, A_2 is the extinction coefficient for the dimeric species, and A_3 is $K_{D(obs.)}$.[15]

The extinction coefficient of the monomer was fixed at 3.0×10^5 $M^{-1} \cdot cm^{-1}$ which was determined by extrapolating of ε_{401} vs. $[NiPPIX]_{total}$ to zero concentration. These spectra, which are shown in Figure 4.7, were recorded from a 10 cm pathlength cell and

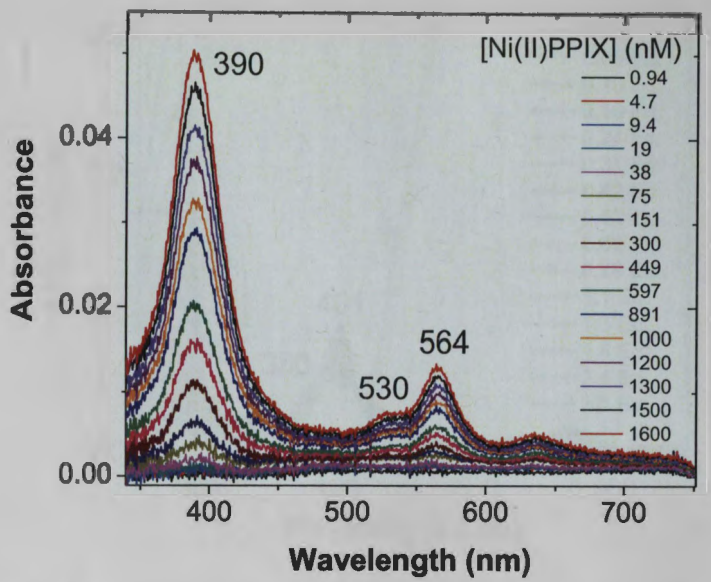

Figure 4.7. UV-visible spectrum of dilute Ni(II)PPIX in aqueous solution. Normalized spectrum of Ni(II)PPIX diluted into aqueous 50 mM Tris-HCl solution at a pH of 8.0 in a 10 cm cell.

normalized. The inset shows the plot of ε_{401} vs. [Ni(II)PPIX]. The extinction coefficient of the dimer, ε_D, and the dimerization constant, $K_{D(obs.)}$, were determined from the least squares fit to be 5.7×10^5 $M^{-1} \cdot cm^{-1}$ and 1.55×10^3, respectively. The deviation of the fit in Figure 4.6 suggests that the speciation of Ni(II)PPIX is more complex than assumed by Equation 4.1.

In an effort to overcome the concentration dependent change in free Ni(II)PPIX speciation during the titration experiments, a second type of titration was performed in which incremental additions of apo-PhuS were made to an aqueous solution of Ni(II)PPIX containing 0.5% DMSO. Based on the dimerization constant determined above, the Ni(II)PPIX concentration was chosen such that >99% of the porphyrin would be monomeric. The resulting spectra which are shown in Figure 4.8, exhibit isosbestic

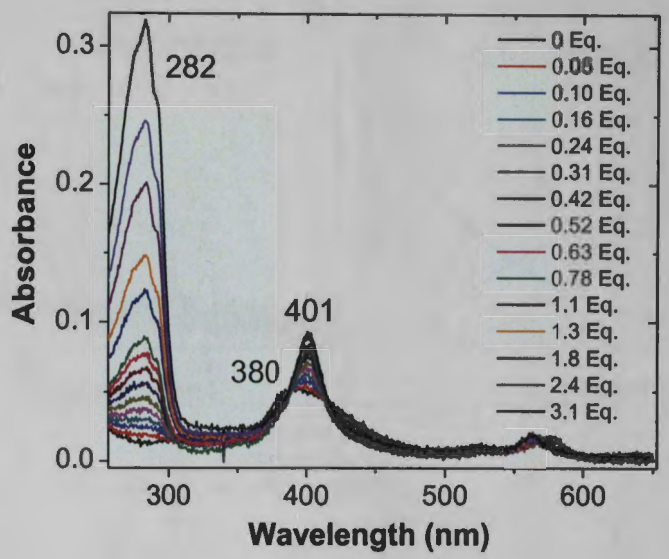

Figure 4.8. UV-visible difference spectrum of PhuS titrated with Ni(II)PPIX. The titration data of PhuS and Ni(II)PPIX from 0 to 3.1 Eq. of PhuS:Ni(II)PPIX. The concentration of Ni(II)PPIX was 1.8 μM and the concentration of stock solution of PhuS was 28 μM. PhuS was titrated into the solution containing Ni(II)PPIX in micromolar increments and the UV-Visible spectrum was taken after equilibrium of the sample was reached. There is an isosbestic point at 388 nm which shows complete conversion of the dimeric species to the monomeric species as the PhuS concentration is increased. This titration reaches saturation of the protein by 1.5 Equivalents of PhuS:Ni(II)PPIX.

behavior consistent with the simple conversion of free Ni(II)PPIX to the Ni(II)PPIX:PhuS complex. This can be seen by the Soret band shift upon increase of PhuS concentration from 380 nm of the aggregated species to 401 nm of the monomeric species. The titrated Ni(II)PPIX spectra (Figure 4.10) were then analyzed by global analysis to determine the stability constant for PhuS:Ni(II)PPIX. Figure 4.9 shows the calculated component spectra, speciation diagram, and titration curves at selected wavelengths for the fit of the titration data in Figure 4.8. Because these titrations took place at around 1.8 μM Ni(II)PPIX, the observed constant for dimerization that was determined was assumed to be accurate. A spectrum of Ni(II)PPIX at a concentration of 0.78 μM was taken in a 10 cm

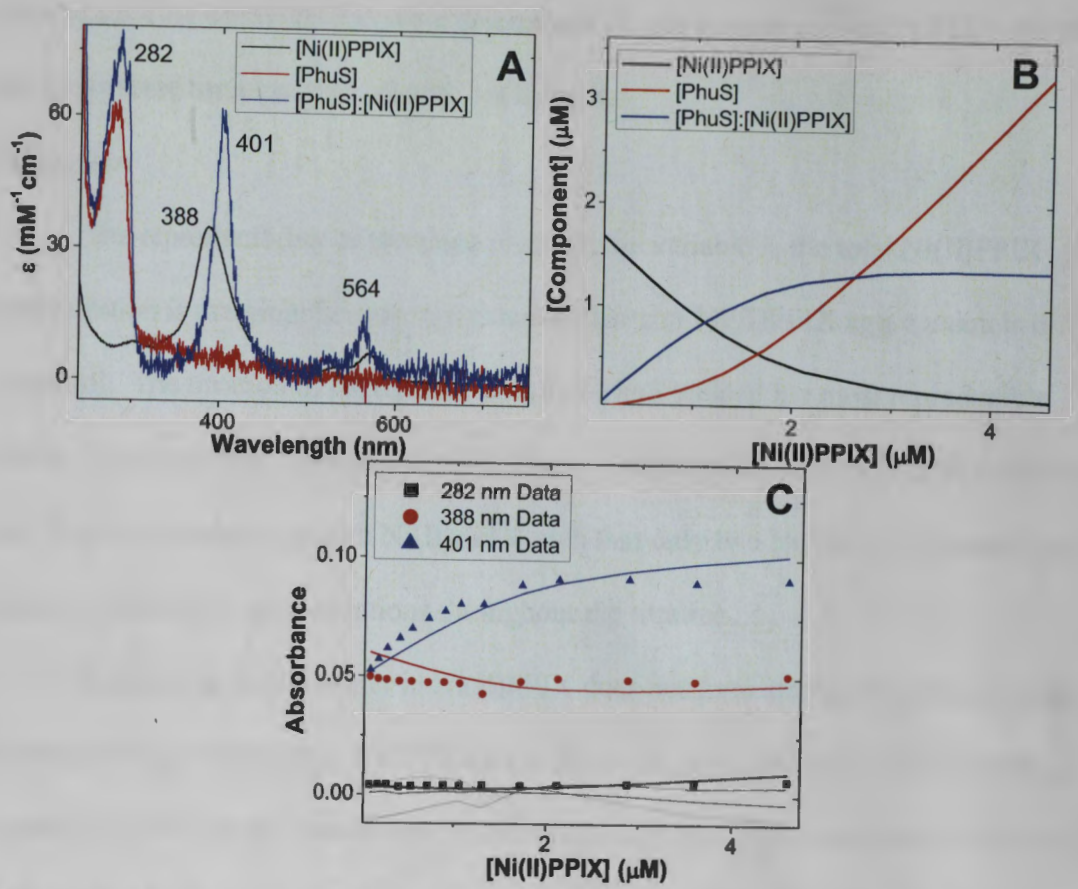

Figure 4.9. Global analysis of PhuS titrated with Ni(II)PPIX. Depicted are the global analysis fitting results for the data in Figure 4.8. (A) Calculated component spectra. (B) Calculated concentration spectra. (C) The titration curves, fit to the data, and calculated residuals show the goodness of fit at the indicated wavelengths. The data were fit to a 1:1 model of [PhuS]:[Ni(III)PPIX].

cell and fixed as the monomer component spectrum in the fit. This spectrum was calculated to be 99% monomeric based on the observed dimerization constant, $K_{D(obs)}$, estimated from the fit in Figure 4.6. The binding constant for PhuS:Ni(II)PPIX was determined to be $3.2(\pm 0.4)\times10^{-7}$ M from three trials. Table 4.1 shows a summary of the

Table 4.1. Average stability constants for the Ni(II)PPIX:PhuS complex.

Type of Titration	Titrant	Fitting Model	Average Stability Constant (M)
PhuS with Ni(II)PPIX	Ni(II)PPIX	Ni(II)PPIX:PhuS	$3.2(\pm 0.6)\times10^{-7}$
Ni(II)PPIX with PhuS	PhuS	PhuS:Ni(II)PPIX	$3.2(\pm 0.4)\times10^{-7}$

average stability constants that were determined for the titration of Ni(II)PPIX with PhuS, and the reverse titration of PhuS with Ni(II)PPIX.

Discussion

The reproducibility of titrations in which the variable is the total Ni(II)PPIX concentration is marginal because the extent and rate of Ni(II)PPIX aggregation is difficult to control. The titration of Ni(II)PPIX with apo-PhuS yielded the most reproducible results. The isosbestic point that occurred upon addition of PhuS to Ni(II)PPIX showed that PhuS was associating with Ni(II)PPIX such that only two Ni(II)PPIX species were present at detectable concentrations throughout the titration.

Because the Ni(II) center in Ni(II)PPIX does not form strong axial ligand bonds, the binding interactions between Ni(II)PPIX and PhuS are likely driven by the nonbonding interactions between the protoporphyrin IX ring and PhuS. This means that when heme binds to PhuS, there are likely significant contributions to the stability of holoPhuS from nonbonding interactions between the porphyrin periphery and the protein, as well as between the iron and protein based axial ligands. It is important to understand how this protein is binding to heme, in order to design an alternative binding agent that could competitively inhibit heme binding. *P. aeruginosa* is an iron-limited bacterium, and PhuS was found to be a necessary in order for the organism to obtain its iron.[16] Therefore finding a more effective binding agent for PhuS than heme would inhibit iron uptake by this organism in the mammalian host medium.

It should be noted that while the results presented here suggest a single Ni(II)PPIX binding site, they do not provide direct evidence that Ni(II)PPIX binds to the same site as hemin. Thus future studies of the complex will aim to determine whether this is the case.

That determination will require other spectroscopic methods, including CD and NMR that directly probe protein structure elements and interactions. Also another way to test if Ni(II)PPIX was bound in the binding pocket of PhuS would be to see if the protein was able to transfer the metalloporphyrin to heme oxygenase.

Once heme binding to PhuS is characterized beyond the metal center ligation, it would also be of future interest to test metalloporphyrins that have properties more ideal for the peripheral binding of the porphyrin ring to PhuS. It appears that Ni(II)PPIX-DME could be toxic to the host since it was found to inhibit β-galactosidase.[17] Therefore although Ni(II)PPIX is useful in characterizing the interactions between the porphyrin periphery and PhuS, its toxicity would likely eliminate it as a potential pharmaceutical agent.

References

1. Carr, H. S.; Tran, D.; Reynolds, M. F.; Burstyn, J. N.; Spiro, T. G., Activation of Soluble Guanylyl Cyclase by Four-Coordinate Metalloporphyrins: Evidence for a Role for Porphyrin Conformation. *Biochemistry* **2002,** *41* (31), 10149-10157.

2. Sanders, J. M., Axial Coordination Chemistry of Metalloporphyrins. In *The Porphyrin Handbook*, Kadish, Ed. Academic Press: London, England, 2000; Vol. 3.

3. Ma, J.-G.; Laberge, M.; Song, X.-Z.; Jentzen, W.; Jia, S.-L.; Zhang, J.; Vanderkooi, J. M.; Shelnutt, J. A., Protein-Induced Changes in Nonplanarity of the Porphyrin in Nickel Cytochrome c Probed by Resonance Raman Spectroscopy. *Biochemistry* **1998,** *37* (15), 5118-5128.

4. Bacarella, A. L.; Grunwald, E.; Marshall, H. P.; Purlee, E. L., The Potentiometric Measurement of Acid Dissociation Constants and pH in the System Methanol-Water: pKa

Values for Carboxylic Acids and Anilinium Ions. *The Journal of Organic Chemistry* **1955,** *20* (6), 747-762.

5. Alden, R. G.; Ondrias, M. R.; Shelnutt, J. A., Influences of .pi.-.pi. complex formation, dimerization, and binding to hemoglobin on the planarity of nickel(II) porphyrins. *Journal of the American Chemical Society* **1990,** *112* (2), 691-697.

6. Stoyanov, S. R.; Yin, C.-X.; Gray, M. R.; Stryker, J. M.; Gusarov, S.; Kovalenko, A., Computational and Experimental Study of the Structure, Binding Preferences, and Spectroscopy of Nickel(II) and Vanadyl Porphyrins in Petroleum. *The Journal of Physical Chemistry B* **2010,** *114* (6), 2180-2188.

7. Housecroft, C., *Inorganic Chemistry.* 3 ed.; Prentice Hall: 2007; p 1136.

8. White, W. I. In *Aggregation of porphyrins and metalloporphyrins*, Academic: 1978; pp 303-39.

9. Alexander, A. E., Monolayers of porphyrins and related compounds. *J. Chem. Soc.* **1937**, 1813-16.

10. Rabinowitch, E.; Epstein, L. F., Polymerization of Dyestuffs in Solution. Thionine and Methylene Blue1. *Journal of the American Chemical Society* **1941,** *63* (1), 69-78.

11. Gallagher, W. A.; Elliott, W. B., Ligand-binding in porphyrin systems. *Ann. N. Y. Acad. Sci.* **1973,** *206*, 463-82.

12. Das, R. R.; Plane, R. A., Dimerization reaction of copper(II), zinc(II), nickel(II) and manganese(III) porphyrin complexes in aqueous solutions[1]. *Journal of Inorganic and Nuclear Chemistry* **1975,** *37* (1), 147-151.

13. Hambright, P., Chemistry of Water Soluble Porphyrins. In *The Porphyrin Handbook*, Kadish, Ed. Academic Press: London, England, 2000; Vol. 3, pp 129-210.

14. Asher, C.; de, V. K. A.; Egan, T. J., Speciation of Ferriprotoporphyrin IX in Aqueous and Mixed Aqueous Solution Is Controlled by Solvent Identity, pH, and Salt Concentration. *Inorg. Chem.* **2009,** *48*, 7994-8003.

15. de Villiers, K.; Kaschula, C.; Egan, T.; Marques, H., Speciation and structure of ferriprotoporphyrin IX in aqueous solution: spectroscopic and diffusion measurements demonstrate dimerization, but not μ-oxo dimer formation. *Journal of Biological Inorganic Chemistry* **2007,** *12* (1), 101-117.

16. Kaur, A. P.; Lansky, I. B.; Wilks, A., The Role of the Cytoplasmic Heme-binding Protein (PhuS) of Pseudomonas aeruginosa in Intracellular Heme Trafficking and Iron Homeostasis. *J. Biol. Chem.* **2009,** *284*, 56-66.

17. Scott, J.; Quirke, J. M. E.; Vreman, H. J.; Stevenson, D. K.; Downum, K. R., Metalloporphyrin phototoxicity. *Journal of Photochemistry and Photobiology B: Biology* **1990,** *7* (2-4), 149-157.